AD_____

AWARD NUMBER: W81XWH-05-1-0007

TITLE: The Role of Siah1-Induced Degradation of β-Catenin in Androgen Receptor Signaling

PRINCIPAL INVESTIGATOR: Shu-ichi Matsuzawa, Ph.D.

CONTRACTING ORGANIZATION: The Burnham Institute
La Jolla, California 92037

REPORT DATE: November 2007

TYPE OF REPORT: Final

PREPARED FOR: U.S. Army Medical Research and Materiel Command
Fort Detrick, Maryland 21702-5012

REPORT DOCUMENTATION PAGE

Form Approved
OMB No. 0704-0188

1. REPORT DATE *(DD-MM-YYYY)*	**2. REPORT TYPE**	**3. DATES COVERED** *(From - To)*
01-11-2007	Final	15 Oct 2004 – 14 Oct 2007

4. TITLE AND SUBTITLE

The Role of Siah1-Induced Degradation of β-Catenin in Androgen Receptor Signaling

5a. CONTRACT NUMBER

5b. GRANT NUMBER
W81XWH-05-1-0007

5c. PROGRAM ELEMENT NUMBER

6. AUTHOR(S)

Shu-ichi Matsuzawa, Ph.D.

E-Mail: smatsuzawa@burnham.org

5d. PROJECT NUMBER

5e. TASK NUMBER

5f. WORK UNIT NUMBER

7. PERFORMING ORGANIZATION NAME(S) AND ADDRESS(ES)

The Burnham Institute
La Jolla, California 92037

8. PERFORMING ORGANIZATION REPORT NUMBER

9. SPONSORING / MONITORING AGENCY NAME(S) AND ADDRESS(ES)
U.S. Army Medical Research and Materiel Command
Fort Detrick, Maryland 21702-5012

10. SPONSOR/MONITOR'S ACRONYM(S)

11. SPONSOR/MONITOR'S REPORT NUMBER(S)

12. DISTRIBUTION / AVAILABILITY STATEMENT
Approved for Public Release; Distribution Unlimited

13. SUPPLEMENTARY NOTES

14. ABSTRACT

The androgen receptor (AR) signaling-pathway plays crucial roles in the growth and progression of prostate cancer cells. Recent studies indicate that β-Catenin physically binds to AR and enhances its transcripitional activity in a ligand dependent manner. p53 has also been implicated in AR signaling because of its ability to induce expression of Siah1, which binds and activates E3 ligase complexes which degrade β-Catenin. In this study, we demonstrated the biological significance and molecular mechanisms by which AR is regulated by the p53-induced Siah1 protein. Moreover, we identified the relevant proteins that are targeted for degradation by Siah1 besides β-Catenin. Thus, enhanced Siah function may suppress the ability of androgen to promote tumor cell growth. Understanding more about the functions of Siah-family proteins may therefore suggest novel strategies for chemoprevention and for improved treatment of prostate cancer.

15. SUBJECT TERMS
No subject terms provided.

16. SECURITY CLASSIFICATION OF:			**17. LIMITATION OF ABSTRACT**	**18. NUMBER OF PAGES**	**19a. NAME OF RESPONSIBLE PERSON**
a. REPORT	**b. ABSTRACT**	**c. THIS PAGE**			USAMRMC
U	U	U	UU	27	**19b. TELEPHONE NUMBER** *(include area code)*

Table of Contents

FINAL REPORT

W81XWH-05-1-0007: The role of Siah1-induced degradation of β-Catenin in androgen receptor signaling.

Shu-ichi Matsuzawa PhD

Introduction:

The androgen receptor (AR) signaling-pathway plays crucial roles in the growth and progression of prostate cancer cells. Recent studies indicate that β-Catenin physically binds to AR and enhances its transcripitional activity in a ligand dependent manner. Mutations that inactivate the p53 gene occur in one-third to half of all human prostate cancers and have been correlated with shorter patient survival. Loss of p53 is known to render tumor cells more resistant to a wide range of anticancer drugs and radiation [1, 2]. It would be highly desirable therefore to have a means of functionally restoring p53 activity in prostate cancers in which this gene has become inactivated. A strategy for accomplishing this is to identify the downstream effectors of p53's actions and to find ways of enhancing their activity in the absence of p53. The human Siah gene is localized on chromosome 16q12-13, a region reported to contain a candidate tumor suppressor gene in various types of cancer, including prostate cancer. Our previous results indicate that over-expression of the Siah1 protein can induce either growth arrest or apoptosis, depending on the cell line tested [3]. The findings suggest that p53-mediated induction of Siah1 expression could play an important role in the mechanisms by which this tumor suppressor inhibits cell proliferation and induces apoptosis. In this study, we designed experiments to test the hypothesis that Siah1 is an important mediator of p53's effects in prostate cancers. If the hypothesis proves to be correct, then the results derived from these studies will lay the groundwork for development of new strategies for restoring p53-like functions in prostate cancers, thus improving therapeutic outcomes for men with carcinoma of the prostate. Our preliminary data also suggest a model by which Siah-family proteins can regulate AR signaling through ubiquitation and degradation of β-Catenin. The central goal of this proposal is to test the validity of this hypothesize model, linking it ultimately to the regulation of tumor cell growth. However, at this point, essentially nothing is known about the relative importance of Siah1 for p53 responses compared to AR target genes. We therefore propose to address the following questions:

1. Is Siah1 a p53 primary response gene in the prostate?
2. What are the mechanisms by which Siah1 inhibits AR activity?
3. Does Siah1 control the sensitivity of human prostate cancer cell lines to anti-androgens in vitro and in xenograph mouse models?
4. What are the relevant proteins that are targeted for degradation by Siah1 besides β-Catenin?

The aims have not changed from the original proposal.

Body:
We have made excellent progress over the entire research period. A brief summary follows:

<u>Aim #1.</u> Examine the effects of p53 on expression of the *Siah1* gene in prostate cells.
The functional p53 binding site was identified in intron 1 of the Siah1 gene.
Using a computer algorithm, we identified nine potential p53-response elements (REs) in intron 1 of the *Siah1* gene (Figure 1A). To explore the possibility that Siah1 is a p53-regulated gene, we cloned four fragments of intron 1 of the *Siah1* gene into a luciferase reporter gene plasmid (named pGL3E-Siah1p53RE-1, 2, 3, and 4) and used transient transfection reporter gene assays to study the effects of p53 on its activity. PPC1, a p53-null prostate cancer cell line was transfected with each of the fragments with or without a plasmid containing wild-type p53. Among the four fragments, only p53RE-3 showed increased luciferase activity in response to p53 (Figure 1B). Since p53RE-3 still includes the potential p53 REs, we made three constructs including each of three p53 REs (named p53RE-3-1, 3-2, and 3-3) and performed luciferase assays (Figure 1C). Among these fragments, only p53RE-3-2 showed increased luciferase activity (Figure 1D). To examine this result, a vector was constructed with four point mutations in the potential p53 binding sequence (Figure 1E) and luciferase activity was assayed. As expected, the mutant did not respond to p53 (Figure 1F). We concluded that the functional p53 RE is located in the region p53RE3-2 of the Siah1 gene intron 1.

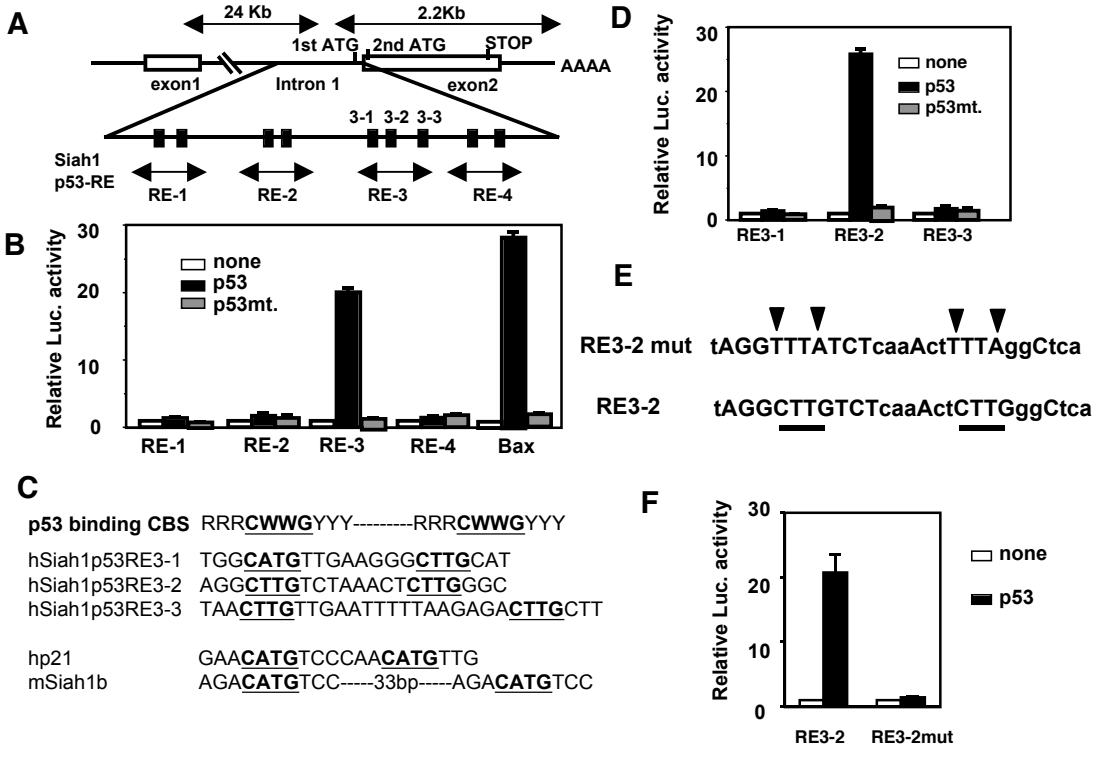

Figure 1. Transcriptional activation by p53 was identified in the intron 1 of the *Siah1* gene. (**A**) Mapping of potential p53 responsive elements (REs) in intron 1 of the *Siah1* gene. Potential p53 binding sites are shown by closed boxes. Lower arrows show the region of various inserts cloned into pGL3-enhancer (pGL3E) vector. The numbers show the name of pGL3E-Siah1p53RE vector. (**B**) Luciferase assay. PPC1 cells were transfected with the same amounts of the different pGL3E-Siah1 promoter vectors (pGL3E-Siah1p53RE-1, 2, 3, and 4), pCMV–p53wt, pCMV–p53mut, and pCMV-β-gal as a transfection efficiency control. pGL3E-Bax vector was used as a positive control. Luciferase activity was measured in cell lysates 24 hrs later and the data were normalized relative to β-galactosidase (mean ± SD; n=3). Lipofectamine™ 2000 (Invitrogen) was used for transfection. The same amounts of plasmid DNA was kept by the addition of empty expression vector. (**C**) Sequences of representative p53-inducible genes and three potential p53REs of the *Siah1* gene inserted into pGL3E-Siah1p53RE3-1, 3-2, and 3-3 vector. The consensus p53 binding sequence (CBS) is show above. (**D**) Luciferase assay using pGL3E-Siah1p53RE3-1, 3-2, and 3-3 promoter vectors. Luciferase activity was measured as described in (C). (**E**) The sequences of potential p53RE in the pGL3E-Siah1p53RE3-2 vector. Mutated points (pGL3E-Siah1p53RE3-2mut) are shown above. (**F**) Luciferase assay using pGL3E-Siah1p53RE3-2 and 3-2mut promoter vectors. Luciferase activity was measured as described in (C).

To further investigate whether the p53 protein is actually able to bind this p53 RE, Electrophoretic Mobility-Shift Assay (EMSA) (Figure 2A) and Chromatin Immunoprecipitation (ChIP) assays (Figure 2B) were performed using MCF7 cells (Figure 2A). In both experiments, we observed actual p53 binding to the p53-RE-3-2. Thus, we concluded that p53 binds directly to the identified p53 RE of Siah1 *in vitro* and *in vivo*.

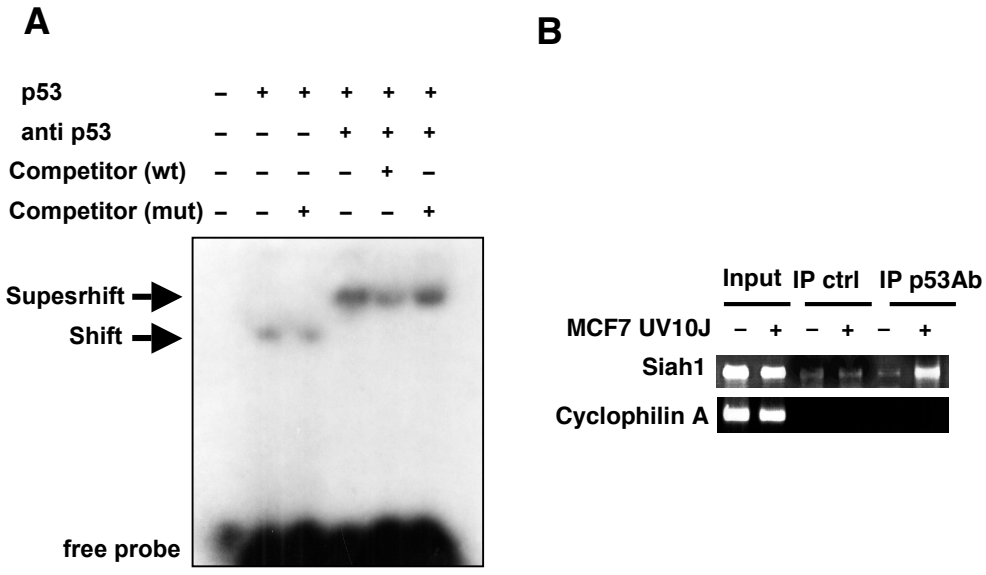

Figure 2. p53 binds directly to the p53RE of *Siah-1 in vitro* and *in vivo*. (**A**) Electrophoretic Mobility-Shift Assay was performed using a 27bp probe including the p53 binding site of *Siah1* (Shown in Figure 2e) and recombinant p53 protein (30 ng, Active Motif) in the presence or absence of anti-p53 antibody (Pab421, Oncogene). Specific binding was determined by adding either unlabeled homologuos probe DNA or mutant DNA (Shown in Figure 2e) at 50-fold molar excess. The positions of the free probe and shifted bands are indicated. (**B**) Chromatin Immunoprecipitation assay was performed as described previously (de Belle, I et al. 2000, BioTechniques). Chromatins from MCF7 cells with or without 24hr after UV-irradiation (10 J/m^2) were immunoprecipitated with (IP p53) or without (IP ctrl) anti-p53 antibody (FL-393, Santa Cruz) overnight at 4°C and followed by incubation with protein A-Sepharose beads (Santa Cruz) for an additional 1hr. After the DNA fragments were purified, PCR amplification was performed using the Siah1 specific primers (5'-AGACATAGCTCATTGCAGCCTTTAC-3' and 5'-

TATTTTGAGGCTTCCACCCAAGC-3') designed to amplify a 280-bp fragment including p53 binding site. The same samples were used for PCR using Cyclophilin A primers (5'-CTCCTTTGAGCTGTTTGCAG-3' and 5'-CACCACATGCTTGCCATCC-3') as a negative control. Total lysate was used as a positive control (input).

Next, to investigate whether Siah1 protein is actually expressed by p53 in cells, RNase protection assays and western bolt analysis were performed using HEK293 cells. Results showed no difference of expression of Siah1 mRNA before and after when HEK293 cells were over-expressed with p53 (Figure 3A). However, a larger size mRNA band was highly expressed after these cells were over-expressed with p53 (especially 12 hours later). Expression of the long type of Siah1 protein, named Siah1L, was also confirmed by western blotting using Siah1-specific antibodies (Figure 3B). The protein sizes of endogenous Siah1 and Siah1L corresponded with transiently transfected Siah1 and Siah1L, respectively using expression vectors. The Siah1L expression was confirmed using the Siah1L specific short interfering RNA (siRNA) vector (pSuppress-Siah1L) (Figure 3C). The protein level of Siah1L was decreased by pSuppress-Siah1L, whereas that of Siah1 did not change. These results indicate that only Siah1L is upregulated in response to p53. Currently, we are analyzing other types of prostate cancer cell lines including LNCaP, PC3, ALVA31, Du145, JCA-1, Tsu-prl and the immortalized prostate epithelial cell line 267β1 cells to contrast the expression of Siah1 and β-Catenin proteins.

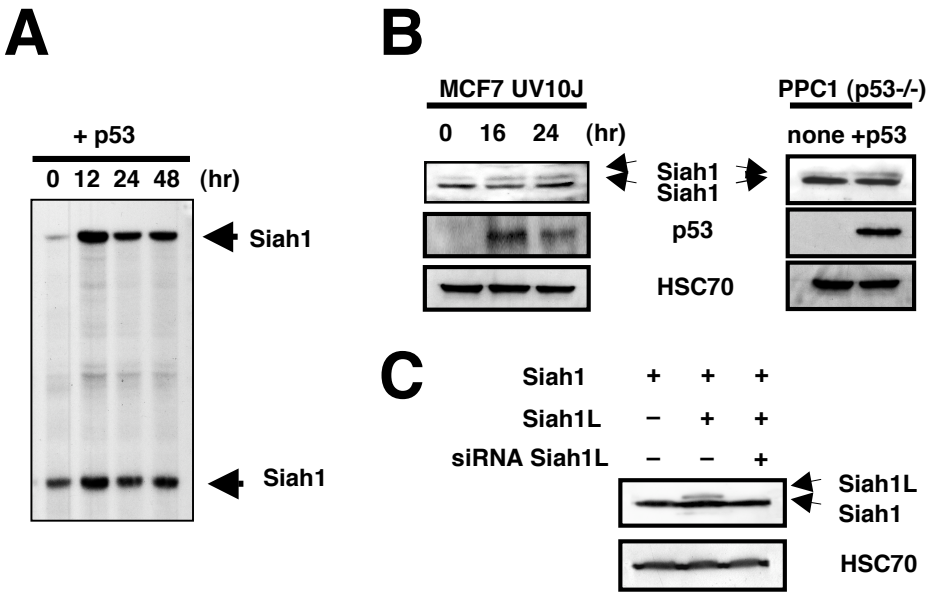

Figure 3. (A) RNase protection assay of *Siah1* mRNA after p53 over-expression. HEK293 cells were transiently transfected with 10 μg of pCMV-p53wt. Total RNAs were extracted from cells at 0, 12, 24 and 48 hr after transfection and *Siah1* RNA expression was measured using a probe containing 324 bp of *Siah1* cDNA. RNase protection assay was performed as previously described [3]. (B) Left; MCF7 cells were treated with UV-irradiation (10 J/m^2). Total proteins were extracted from cells at 0, 16, 24 hr after transfection. Right; PPC1 cells were transiently transfected with empty vector or pCMV-p53wt. Cells were lysed with RIPA buffer (50mM Tris-HCl, 150mM NaCl, 1% NP-40, 0.5% DOC, 0.1% SDS). The same amounts of cells lysates (60 μg per lane) were analyzed by immunoblotting, using antibodies specific for Siah1 (N-15, Santa Cruz), p53 (Pab421, Oncogene). The membrane was reprobed with goat anti-HSC70 antibody (K-19, Santa Cruz) as a control. (**C**) PPC1 cells were transiently transfected with pcDNA3-Siah1, pcDNA3-Siah1L, and pSuppress-Siah1L (siRNA-Siah1L) in various combinations, as indicated. Empty

pcDNA3 and pSuppress vectors were used as controls. After 24 hrs, the lysates (60 μg per lane) were analyzed by immunoblotting, using antibodies specific for Siah1. The membrane was reprobed with goat anti-HSC70 antibody as a control. The cDNAs encoding human *Siah1* and *Siah1L* were generated by PCR as described previously [3]. pSuppress, an siRNA-expressing plasmid, was kindly provided by D. Billadeau (Mayo Clinic, Rochester, MN). The following *Siah1L* target sequence was inserted: 5'-CTCCTGCCTCCTTATGTAT-3'.

These results suggest that *Siah1L* is a direct transcriptional target of p53 and involved in p53-regulated pathway. This aim had been completed and a manuscript is being prepared.

<u>Aim #2</u>. Determine the importance of p53-induced degradation of β-Catenin in Siah-mediated suppression of AR activity.

Androgen plays an important role in progressing prostate cancers (CaP) through androgen receptor (AR)-mediated signaling. Recent studies indicate that β-Catenin binds directly to AR and enhances its activity [4-9]. On the other hand, p53 is reported to suppress AR activity indirectly [10], however, its functional role is still unclear. To determine whether the degradation of β-Catenin by Ebi is important for Siah-mediated suppression of AR activity, a dominat-negative Ebi mutant was constructed which fails to bind Skp1 but still binds to β-catenin. As expected, over-expression of the mutant Ebi abrogated the Siah1-induced suppression of AR activity, suggesting that Ebi is essential for the Siah1–induced suppression of AR activity (Figure 4A).

To further investigate whether Siah1L is necessary for p53-dependent regulation of AR activity, we used Siah1L-specific siRNA. AR activity was measured by luciferase assay using PPC1 cells transfected with pMMTV (AR responsive luciferase reporter plasmid). p53 over-expression resulted in a decrease of AR activity (Figure 4B). However, introduction of Siah1L siRNA failed to suppress AR activity by p53 (Figure 4B). These data suggest that Siah1L is important for p53-depenpent β-catenin degradation pathway.

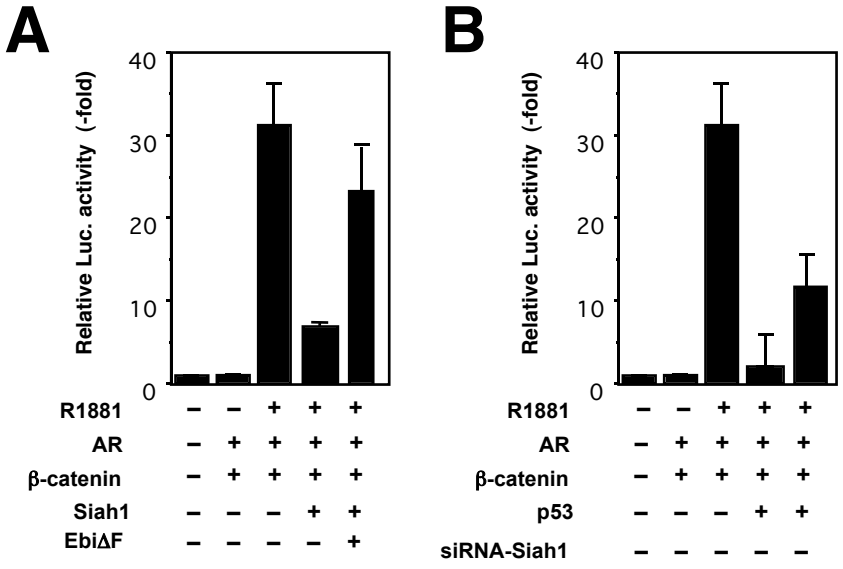

Figure 4. PPC1 cells were transiently transfected with pMMTV-Luc plasmid that contains an AR responsive element cloned upstream of a luciferase reporter gene together with pCMV-βGal as a transfection-efficiency control and the indicated plasmids encoding AR-encoding plasmid pSG5-AR(AR),

β-Catenin, p53, Siah1, Ebi (EbiΔF) or pSuppress-Siah1L (siRNA-Siah1L). Twenty-four hours after transfection, cells were stimulated with 1 nM R1881. Cell extracts were prepared and assayed for luciferase and β-galactosidase activity at 48 h. Data were normalized using β-galactosidase, and results are expressed as –fold transactivation relative to cells transfected with the reporter gene alone (mean ± S.D.; n=3).

Next, we analyzed the effect of this pathway using various p53 wild-type (WT) and p53 mutated (MT) CaP cell lines. AR activity was measured by luciferase assay using PPC1 cells transfected with pMMTV (AR responsive luciferase reporter plasmid). Over-expression of β-Catenin enhanced AR activity in p53WT, but not in p53MT CaP cell lines (Figure 5). Thus, our findings suggest that Siah1 regulates AR-mediated signaling in CaP cell lines through p53-induced β-Catenin degradation and might be one of key proteins for CaP progression.

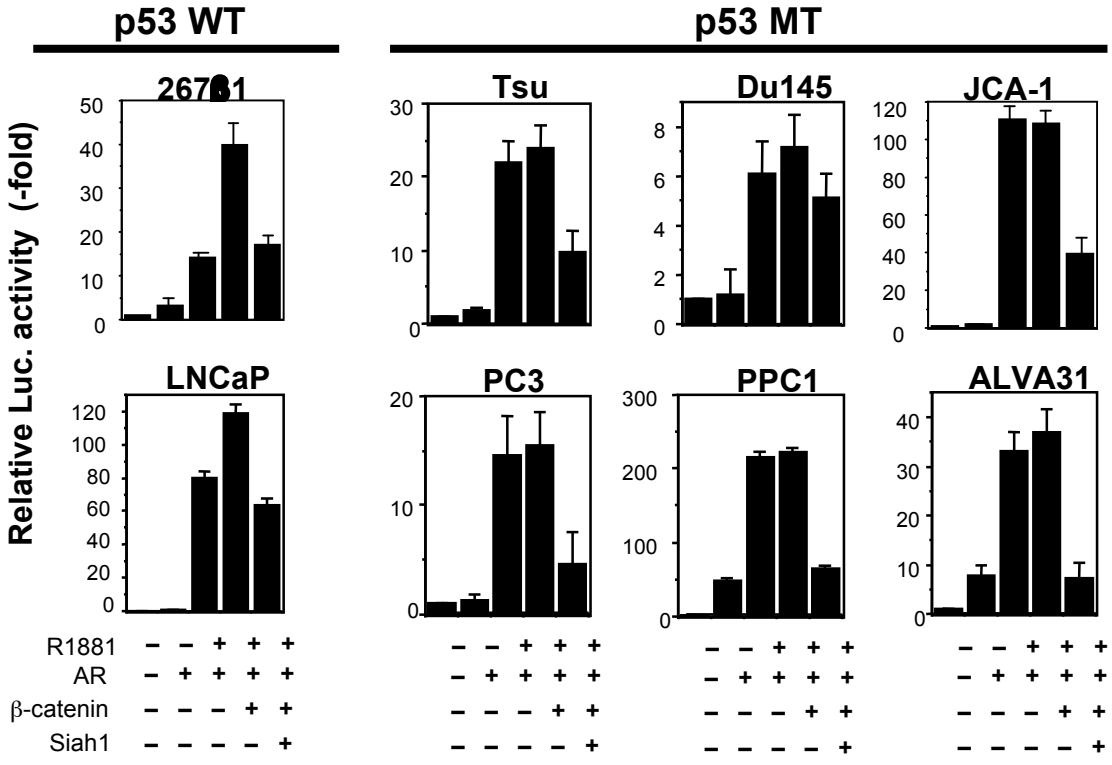

Figure 5. Dependency of p53 on AR activation by β-Catenin.
The AR-encoding plasmid pSG5-AR(AR) was co-transfected into p53 wild-type prostate cancer cells (p53 WT) and p53 mutated prostate cancer cells (p53 MT) with pMMTV-luc reporter plasmid, pCMV-βGal and plasmid encoding β-Catenin and Siah1 as indicated. Twenty-four hours after transfection, cells were stimulated with 1 nM R1881. Cell extracts were prepared and assayed for luciferase and β-galactosidase activity at 48 h. Data were normalized using β-galactosidase, and results are expressed as –fold transactivation relative to cells transfected with the reporter gene alone (mean ± S.D.; n=3).

These results suggest that Siah1 is necessary for p53-dependent regulation of AR activity. This aim has been completed and a manuscript is being prepared.

<u>Aim #3.</u> Explore the effects of Siah1 on the control of sensitivity of human prostate cancer cell lines to anti-androgens in vitro and in xenograph mouse models.
We have attempted to establish stable cell lines that express TET-inducible Siah1. However, we could not obtain the cell line. We also had tried to use other expression systems, such as several metal-inducible systems, but none of them worked successfully. One major problem was a leaking expression of Siah1 in these the prostate cancer cell lines since Siah1 expression, even low amount, induced apoptosis in the cells. Therefore, we could not proceed to the experiment using xenograph mouse model.

<u>Aim #4</u>. What are the mechanisms by which Siah1 suppresses androgen receptor activity?

To identify potential targets of Siah1, yeast two-hybrid screens of cDNA libraries made from prostate cancer cell lines were performed using the human Siah1 protein as a bait. This effort has resulted in identification of a known Siah-binding protein AF4 [4, 5] and a novel protein that we call SIP2, for Siah1 Interacting Protein 2 (Figure 6).

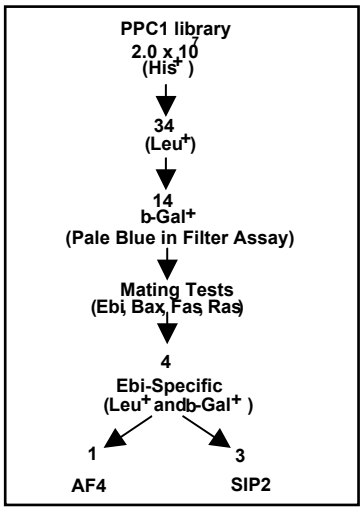

Figure 6. <u>Identification of SIP2 as a candidate Siah1-binding protein by two-hybrid cDNA library screening</u>. Library screening by the yeast two-hybrid method was performed as described [3] using pGilda encoding human Siah1 as a bait, cDNA libraries derived from PPC1, and EGY48 strain yeast. Cells were grown in either YPD medium with 1% yeast extract, 2% polypeptone, and 2% glucose, or in Burkholder's minimal medium (BMM) fortified with appropriate amino-acids as described previously [3]. Transformations were performed by a LiCl method using 0.1 mg of pJG4-5-cDNA library DNA, and 5 mg of denatured salmon sperm carrier DNA. Clones that formed on Leu-deficient BMM plates containing 2% galactose / 1% raffinose were transferred to BMM plates containing leucine and 2% glucose, and filter assays were performed for β-galactosidase measurements. The specificity of two-hybrid interactions mediated by candidate cDNA clones was evaluating by mating with RFY206 cells, which contained one of 4 different indicator pGilda plasmids encoding the following LexA bait proteins: Ebi, Bax (1-171), Fas (191-335) or v-Ras.

Siah1 binds a novel protein SIP2. Among the other cDNA clones identified in the two-hybrid screen described above were 3 that encoded a novel protein we have termed SIP2, for Siah1 Interacting Protein 2.

SIP2 binds specifically to Siah1 in yeast two-hybrid assays. The minimal length cDNA clones that permitted positive interactions in yeast two-hybrid experiments encompassed the C-terminal 151 amino acids of SIP2. A search of the homology database shows that there is no homology against known proteins. Interestingly, at least 3 putative Siah-binding motifs [13] were identified in the C-terminal region of SIP2 protein (Figure 7). Site-directed mutagenesis of these Siah-binding motifs showed loss of binding of Siah1 to SIP2 by yeast 2-hybrid system (data not shown). Interaction of SIP 2 with Siah1 has been confirmed by in vitro binding experiments and co-immunoprecipitation assays in which epitope tagged Siah1 and SIP2 proteins were co-expressed in 293T cells (Figure 8).

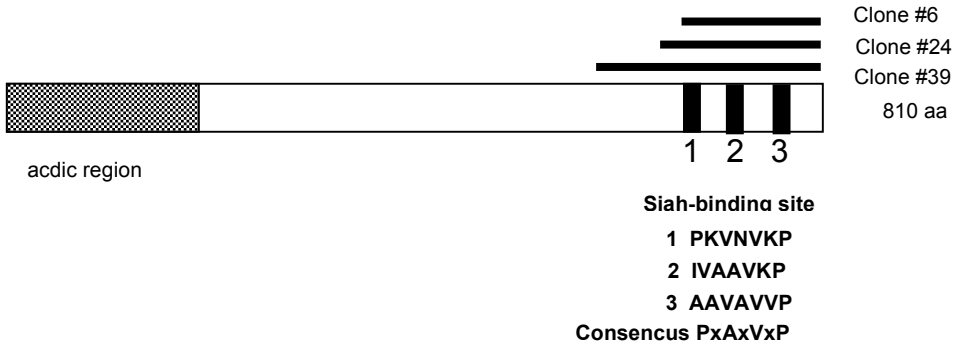

Figure 7. Structure of SIP2 protein.

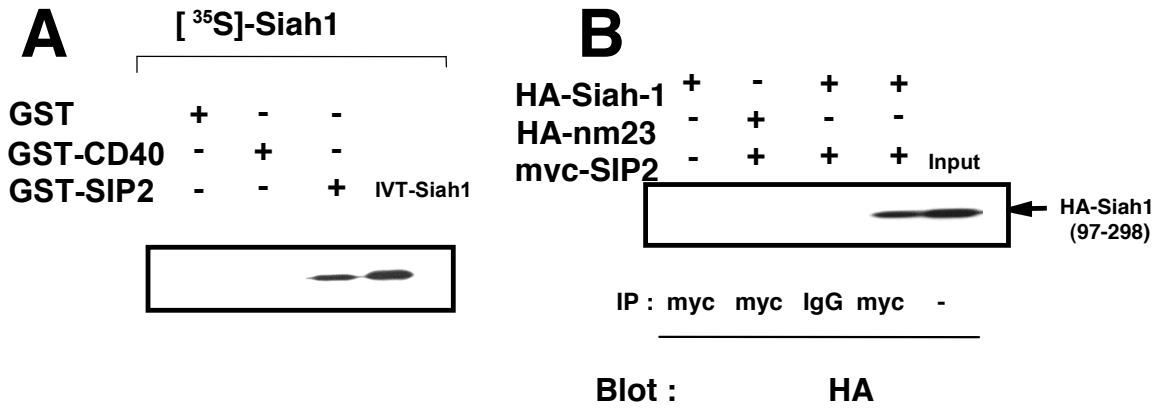

Figure 8. **Analysis of Siah1 and SIP2 interactions.** **(A)** Radiolabeled Saih1 protein was produced by in vitro translation (IVT) in reticulocyte lysates in the presence of ^{35}S-L-methionine. ^{35}S-Siah1 was incubated with 1 μg of GST, GST-CD40 cytosolic domain, or GST-SIP2 proteins immobilized on glutathione-Sepharose. After 1 hr, beads were washed extensively and analyzed by SDS-PAGE/autoradiography. As a control, 0.1 volume of input in vitro translated (IVT) ^{35}S-Siah1 was loaded directly in the same gel. **(B)** 293T cells were transfected with plasmids producing HA-tagged Siah1 or nm23, myc-tagged SIP2, in various combinations. Controls (-) represent cells transfected with HA or myc-tag pcDNA3 lacking a cDNA insert. Lysates were either loaded directly in gels or subjected to immunoprecipitation using either

anti-HA antibody or control IgG. Immune-complexes were analyzed by SDS-PAGE/immunoblotting using anti-myc-tag antibody with ECL-based detection.

The region in Siah1 required for SIP2 binding was preliminarily mapped to the C-terminus of Siah1 (Figure 9), based on yeast two-hybrid assays using a panel of Siah-1 truncation mutants constructed in our previous work [13]. These two-hybrid assay results were confirmed by in vitro protein binding assays, using GST-SIP2 (659-810) fusion protein for binding to in vitro translated full-length Siah1, Siah1 (ΔRING), or Siah-1 (ΔC) proteins (not shown). Thus, the N-terminal RING domain (which binds UBCs) is not required for SIP2 binding. We therefore speculate that Siah can bridge UBCs to APC, using its N-terminal domain to bind UBC and its C-terminal domain to bind APC.

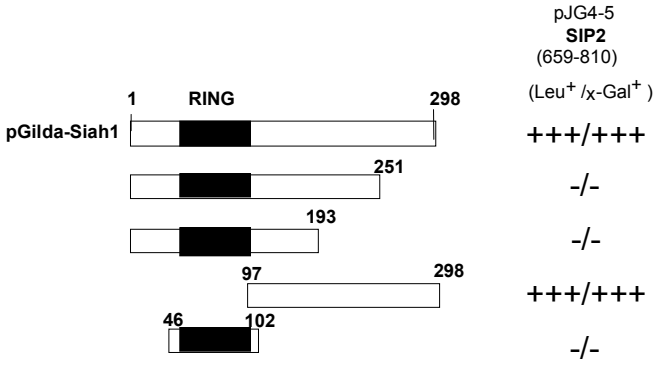

Figure 9. SIP2 Binds Carboxyl-Domain in Siah1. Yeast two-hybrid experiments were performed by transforming EGY48 (strain) cells. Wild-type Siah1 or various mutants as indicated were expressed from the plasmid pGilda and tested for interactions with SIP2, which were expressed from the pJG4-5 plasmid. Interactions were detected by trans-activation of *LEU2* or β-galactosidase reporter genes. Growth on leucine-deficient medium at 30°C was examined 4 days later.

Siah1 regulates degradation of SIP2. We speculated that SIP2 might become a target of Siah1-induced protein degradation. To preliminarily explore this hypothesis, a myc-tagged SIP2 protein was expressed in PPC1 cells (a) alone, (b) with full-length Siah1, or (c) with a Siah1(ΔRING) mutant that fails to bind UBCs. Co-expression of Siah1 with SIP2 resulted in a marked decrease in the levels of SIP2 protein (Figure 10). In contrast, the Siah1(ΔRING) protein did not reduce SIP2 levels in cells.

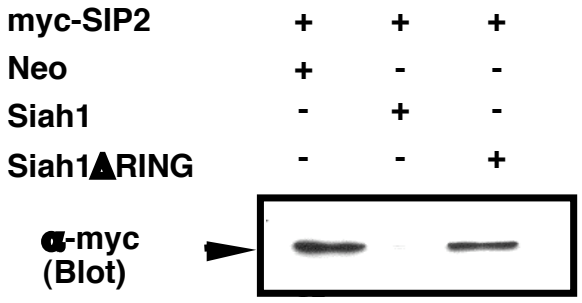

Figure 10. Siah1 regulate SIP2 levels. PPC1 cells were transiently transfected with 0.2 mg pEGFP and plasmids encoding FLAG-Siah1 (0.2 μg), FLAG-Siah1ΔR (0.5 μg), or myc-SIP2 (0.5 μg) in various combinations, as indicated (total DNA amount normalized). After 24 h, cell lysates were prepared from duplicated dishes of transfectants, normalized for total protein content (40 μg per lane), and analyzed by SDS-PAGE/immunoblotting using antibodies specific for myc with ECL-based detection.

Explore whether alterations in the levels of Siah-family proteins occur during the pathogenesis of prostate cancer. To begin our studies of the regulation of SIP2 gene expression, we developed RNAase protection assays that allow for specific detection of each of the three known members of the Siah-family. We have first analyzed the level of expression of Siah-family genes in different tumor cell lines. The level of SIP2 expression was assayed by RNase protection assay in several prostate tumor lines. The results obtained demonstrated that the SIP2 gene was expressed in all prostate cancer cell lines. However, significant alterations in mRNA levels of SIP2 had not been observed in prostate cancer cell lines compared with other cancer cell lines or normal cell lines.

We have begun to raise mouse monoclonal antibodies specific for SIP2 using these reagents to assess the expression of SIP2 proteins in prostate cancer cell lines and prostate tumors by immunoblotting and immunohistochemistry

Functional analysis of SIP2 in AR signaling pathway.

To explore the functional consequences of Siah1/SIP2 interactions, we examined the effect of the SIP2 proteins on AR activity. AR activity was measured by luciferase assay using LNCap cells transfected with plasmids encoding β-catenin, Siah1 or SIP2 in various combinations. However, induction of SIP2 did not affect on the β-catenin-activated AR activity. Furthermore, over-expression of the SIP2 had no influence on the Siah1-induced suppression of AR activity. Further analysis will be needed to determine the function of SIP2 using siRNA or gene targeting mouse in the future.

Key Research Accomplishment:

We have made excellent progress in the first year of funding towards accomplishing these goals. Two manuscripts are being prepared regarding Aim#1 and #2. However, we could not complete Aim#3 with technical problem. We also obtained a potential target of Siah1 termed SIP2. To explore the functional consequence of Siah1/SIP2 interection, further analysis will be needed.

Reportable Outcomes:

Publication

1. Fukushima T, Zapata JM, Singha NC, Thomas M, Kress C, Krajewska M, Krajewski S, Ronai Z, Reed JC, and **Matsuzawa S**. Critical function for SIP, a ubiquitin E3 ligase component of the β-Catenin degradation pathway, for thymocyte development and G1 checkpoint. ***Immunity*** 2006. 24:29-39.

Meeting Abstract

1. Fukushima T, Zapata JM, Krajewska M, Krajewski S, Reed JC, **Matsuzawa S** Critical function for p53-induced b-Catenin degradation at G1 checkpoint during cell cycle progression. Proc. Am. Assoc. Cancer Res., 46-607, 2005.

2. Fukushima T, **Matsuzawa S**, Kress C, Bruey JM, Krajewska M, Lefebvre, S, Zapata JM, Ronai Z, and Reed JC. Ubiquitin-conjugating enzyme Ubc13 is a critical component of TRAF-mediated inflammatory responses. ASH Annual Meeting Abstracts, 108:337a, 2006

Conclusions:

We have determined that *Siah1* is a primary response gene for p53. We have also demonstrated that Siah1-specific siRNA showed down-regulation of AR activity by p53. These findings suggest that Siah1 is a critical regulator of AR signaling and there are new strategies for restoring tumor suppressive pathways lost in cancers that have suffered p53 inactivation.

References:

1. Anthoney, D.A., McIlwrath, A.J., Gallagher, W.M., Edlin, A.R., and Brown R. Microsatellite instability, apoptosis, and loss of p53 function in drug-resistant tumor cells. Cancer Res. (1996) 56:1374-1381.
2. Sanchez-Prieto, R., Lleonart, M., Ramon, Y., and Cajal, S. Lack of correlaqtion between p53 protein level and sensitivity of DNA-damaging agents in keratinocytes carrying adenovirus E1a mutants. Oncogene (1995) 11: 675-682.
3. Matsuzawa, S. and J.C. Reed, Siah-1, SIP, and Ebi collaborate in a novel pathway for β-catenin degradation linked to p53 responses. Mol Cell (2001) **7**: 915-926.
4. Truica, C.I., S. Byers, and E.P. Gelmann, β-catenin affects androgen receptor transcriptional activity and ligand specificity. Cancer Res. (2000) 60:4709-4713.
5. Yang, F., Li, X., Sharma, M., Sasaki, C.Y., Longo, D.L., Lim, B., Sun, Z. Linking β-catenin to androgen-signaling pathway. J. Biol. Chem. (2002) 277:11336-11344.
6. Pawlowski, J.E., Ertel, J.R., Allen, M.P., Xu, M., Butler, C., Wilson, E.M., Wierman, M.E. Liganded androgen receptor interaction with β-catenin: nuclear co-localization and modulation of transcriptional activity in neuronal cells. J Biol Chem. (2002) 277: 20702-20710.
7. Mulholland, D.J., Cheng, H., Reid, K., Rennie, P.S., Nelson, C.C. The androgen receptor can promote β-catenin nuclear translocation independently of adenomatous polyposis coli. J. Biol. Chem. (2002) 277:17933-17943.
8. Song, L.N., Herrell, R., Byers, S., Shah, S., Wilson, E.M., Gelmann, E.P. β-catenin binds to the activation function 2 region of the androgen receptor and modulates the effects of the N-terminal domain and TIF2 on ligand-dependent transcription. Mol. Cell. Biol. (2003) 23:1674-1687.
9. Chesire, D.R. and W.B. Isaacs, β-catenin signaling in prostate cancer: an early perspective. Endocr. Relat. Cancer (2003)10:537-560.
10. Shenk, J.L., Fisher, C.J., Chen, S.Y., Zhou, X.F., Tillman, K., Shemshedini, L. p53 represses androgen-induced transactivation of prostate-specific antigen by disrupting hAR amino- to carboxyl-terminal interaction. J. Biol. Chem. (2001) 276:38472-38479.
11. Oliver, P.L., Bitoun, E., Clark, J., Jones, E.L., Davies, K.E. Mediation of Af4 protein function in the cerebellum by Siah proteins. Proc. Natl. Acad. Sci. USA. (2004) 101:14901-14906.
12. Bursen, A., Moritz, S., Gaussmann, A., Moritz, S., Dingermann, T., and Marschalek, R. Interaction of AF4 wild-type and AF4.MLL fusion protein with SIAH proteins: indication for t(4;11) pathobiology? Oncogene (2004) 19:6237-6249.
13. Santelli, E., Leone, M., Li, C., Fukushima, T., Preece, N.E., Olson, A.J., Ely, K.R., Reed, J.C., Pellecchia, M., Liddington, R.C., Matsuzawa, S. Structural analysis of Siah1-Siah-interacting protein interactions and insights into the assembly of an E3 ligase multiprotein complex. J. Biol. Chem. (2005) 280:34278-34287.

List of Personnel:

Shu-ichi Matsuzawa Ph.D. Principal Investigator:

Dr Matsuzawa has been served as the PI for the all project. Dr. Matsuzawa is responsible for the daily supervision of the project personnel and provided the overall scientific and administrative direction for the project. He is also responsible for progress reports and writing or editing of all research reports submitted for publication.

Toru Fukushima M.D., Ph.D., Post-Doctoral Fellow (40% effort):

Dr Fukushima is a post-doctoral fellow in the Matsuzawa laboratory who generated most of the data regarding the effects of Siah1 on androgen receptors. He led the investigations of the mechanism of Siah1 in androgen receptor signaling pathway.

John C. Reed, M.D., Ph.D. (Collaborator and Advisor):

Dr Reed is a President/CEO at the Burnham Institute. Dr. Reed has provided Dr. Matsuzawa's group with reagents and advised for multiple aspects of the work on Siah effects on steroid hormone receptors. He served as a non-paid collaborator and advisor for the project.

Stan Krajewski M.D., Ph.D. (Collaborator and Advisor):

Dr. Krajewski is a longstanding collaborator of Dr. Matsuzawa and expert pathologist Dr Krajewski served as a non-paid collaborator and advisor for the project.

Appendices:

1. Reprint

   Fukushima T, Zapata JM, Singha NC, Thomas M, Kress C, Krajewska M, Krajewski S, Ronai Z, Reed JC, and **Matsuzawa S**. Critical function for SIP, a ubiquitin E3 ligase component of the β-Catenin degradation pathway, for thymocyte development and G1 checkpoint. ***Immunity*** 2006. 24:29-39.

Immunity 24, 29–39, January 2006 ©2006 Elsevier Inc. DOI 10.1016/j.immuni.2005.12.002

Critical Function for SIP, a Ubiquitin E3 Ligase Component of the β-Catenin Degradation Pathway, for Thymocyte Development and G1 Checkpoint

Toru Fukushima,[1] Juan M. Zapata,[1] Netai C. Singha,[1] Michael Thomas,[1] Christina L. Kress,[1] Maryla Krajewska,[1] Stan Krajewski,[1] Ze'ev Ronai,[1] John C. Reed,[1] and Shu-ichi Matsuzawa[1,*]
[1] Burnham Institute for Medical Research
10901 North Torrey Pines Road
La Jolla, California 92037

Summary

β-catenin has been implicated in thymocyte development because of its function as a coactivator of Tcf/LEF-family transcription factors. Previously, we discovered a novel pathway for p53-induced β-catenin degradation through a ubiquitin E3 ligase complex involving Siah1, SIP (CacyBP), Skp1, and Ebi. To gain insights into the physiological relevance of this new degradation pathway in vivo, we generated mutant mice lacking SIP. We demonstrate here that *SIP*$^{-/-}$ thymocytes have an impaired pre-TCR checkpoint with failure of *TCRβ* gene rearrangement and increased apoptosis, resulting in reduced cellularity of the thymus. Moreover, the degradation of β-catenin in response to DNA damage is significantly impaired in *SIP*$^{-/-}$ cells. *SIP*$^{-/-}$ embryonic fibroblasts show a growth-rate increase resulting from defects in G1 arrest. Thus, the β-catenin degradation pathway mediated by SIP defines an essential checkpoint for thymocyte development and cell-cycle progression.

Introduction

β-catenin, an important regulator of cell-cell communication and embryonic development, associates with and regulates the function of Tcf/LEF-family transcription factors (Peifer and Polakis, 2000). Conditional degradation of β-catenin represents a central event in Wnt signaling pathways controlling cell fate and proliferation (Peifer and Polakis, 2000). Interaction of Wnt-ligands with frizzled-family receptors transduces signals that suppress GSK3β activity, via mechanisms requiring APC, Axin, and other proteins. Suppression of GSK3β reduces phosphorylation of β-catenin, thus eliminating binding of F box protein β-TrCP/Fbw1 and resulting in β-catenin accumulation due to reduced ubiquitin-mediated proteolysis (Hart et al., 1999; Kitagawa et al., 1999b; Latres et al., 1999; Winston et al., 1999). β-catenin accumulation facilitates its translocation to a nucleus where it collaborates with Tcf/LEF-family (high-mobility group) transcription factors to activate expression of target genes important for cell proliferation, such as *c-myc* (He et al., 1998) and *cyclin D1* (Tetsu and McCormick, 1999). Mutations in β-catenin inappropriately activate various transcription factors, thereby promoting malignant transformation (Peifer and Polakis, 2000; Polakis, 2000).

*Correspondence: smatsuzawa@burnham.org

Genotoxic stress triggers activation of checkpoints that delay cell-cycle progression (Abraham, 2001; Zhou and Elledge, 2000). Defective cell-cycle checkpoints lead to genomic instability and a predisposition to cancer. Cell-proliferation arrest is also required to allow T cell receptor (TCR) genes rearrangement in the thymus, which is a crucial step in T cell development (Borowski et al., 2002; Hoffman et al., 1996). This checkpoint critically depends on stage-specific signals derived from the thymic microenvironment. In this regard, β-catenin has been implicated in T cell development, where it plays an essential role in differentiation of $CD4^-CD8^-$ double-negative to $CD4^+CD8^+$ double-positive thymocytes (Ioannidis et al., 2001; Mulroy et al., 2003; Xu et al., 2003). Moreover, expression of active β-catenin in the thymus results in the generation of T cells lacking mature T cell antigen receptors (TCRs) and impairs thymocyte survival (Gounari et al., 2001).

Upon DNA damage, p53 is stabilized and activated via posttranslational mechanisms, leading to growth arrest or apoptosis (Hall and Lane, 1997; Hartwell and Kastan, 1994; Reed, 1996; Vogelstein et al., 2000). The p53 protein has been shown to transactivate a wide variety of target genes, including the cell-cycle inhibitor $p21^{waf-1}$ (El-Deiry et al., 1993; Harper et al., 1993). Upregulation of $p21^{waf-1}$ inhibits cyclin-dependent kinases, particularly those that function during the G1 phase of the cell cycle. However, *waf-1*-deficient mice develop normally, and fibroblasts derived from $p21^{waf-1}$-deficient mouse embryos are only partially defective in their ability to undergo cell-cycle arrest in response to DNA damage (Brugarolas et al., 1995; Deng et al., 1995). These observations suggest the existence of an alternative $p21^{waf-1}$-independent pathway through which p53 can suppress cell proliferation.

Previously, we and others observed that β-catenin is downregulated by activated p53 (Liu et al., 2001; Matsuzawa and Reed, 2001; Sadot et al., 2001). Furthermore, we discovered that this β-catenin degradation pathway is mediated by a series of protein interactions involving Siah1, SIP (CacyBP), Skp1, APC, and Ebi, an F box protein that binds β-catenin independently of the phosphorylation sites recognized by β-TrCP/Fbw1 (Liu et al., 2001; Matsuzawa and Reed, 2001). Siah family proteins bind ubiquitin-conjugating enzymes and target proteins for proteasome-mediated degradation (Reed and Ely, 2002). We identified a novel Siah-interacting protein (SIP), an SGT1-related molecule that provides a physical link between Siah-family proteins and the SCF ubiquitin E3 ligase component Skp1 (Kitagawa et al., 1999a; Matsuzawa et al., 2003; Santelli et al., 2005). Expression of Siah1 is induced by p53 (Iwai et al., 2004; Matsuzawa et al., 1998), thereby linking genotoxic injury to destruction of β-catenin, thus reducing activity of β-catenin-binding Tcf/LEF transcription factors and contributing to cell-cycle arrest (Matsuzawa and Reed, 2001).

To gain insights into the function of SIP in p53-induced β-catenin degradation in vivo, we generated *SIP* knockout mice. First, we identified a specific stage of T cell development at which SIP is required for T cell

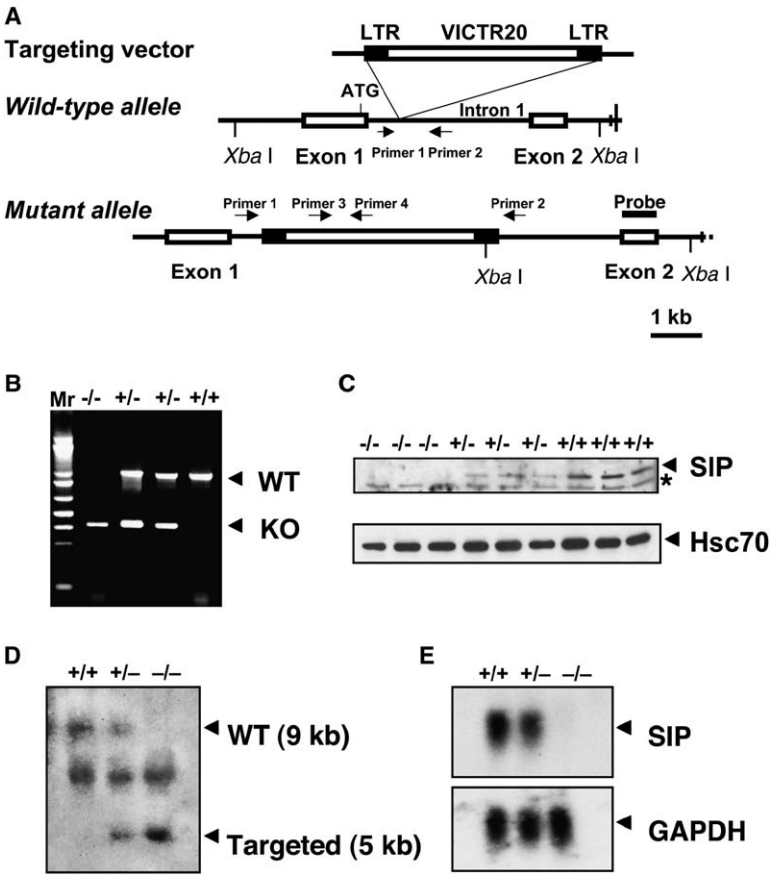

Figure 1. Targeted Disruption of Mouse *SIP* Gene

(A) The targeting vector VICTR20, wild-type *SIP* allele, and targeted allele are depicted. The vector was targeted to the first intron of the *SIP* locus. The closed rectangles denote exons 1 and 2 of *SIP*, and the open rectangles denote the retroviral LTRs.

(B) PCR analysis of genomic DNA extracted from mouse tails. Primers were designed to amplify the regions of wild-type and mutant alleles. PCR products of wild-type (WT) and mutated (KO) alleles are shown. The genotypes of mice are presented above the lane.

(C) Immunoblot analysis of extracts from $SIP^{-/-}$, $SIP^{+/-}$, and $SIP^{+/+}$ mouse embryonic fibroblasts (MEFs). Whole-cell lysates of MEFs were prepared from the indicated mouse genotypes and subjected to SDS-PAGE and immunoblotting with rabbit anti-SIP antibody and then reprobed with goat anti-Hsc70 antibody. Bands corresponding to SIP and Hsc70 are indicated. Asterisk indicates nonspecific bands.

(D) Southern-blot analysis of genomic DNA extracted from MEFs of the indicated SIP genotypes. The DNA was digested with XbaI and subjected to hybridization with the probe shown in (A). The expected sizes of the bands corresponding to WT and KO alleles are indicated.

(E) Northern-blot analysis of total RNA isolated from MEFs of the indicated SIP genotypes. Hybridization was performed with mouse *SIP* and *GAPDH* cDNA probes.

differentiation, mimicking the previously reported effect of constitutive expression of β-catenin in thymocytes. Second, we show that embryonic fibroblasts derived from mice lacking SIP are deficient in their ability to arrest in G1 following DNA damage. These data underline the essential role of SIP as a component of the p53-regulated pathway that controls β-catenin levels in vivo and regulates the thymocyte development and G1 cell-cycle checkpoint.

Results

Generation of SIP-Deficient Mice

The murine ortholog of *SIP* was initially characterized as a calcyclin-binding protein (CacyBP) (Filipek and Kuznicki, 1998; Filipek and Wojda, 1996) and resides on chromosome 1H1. By searching the Omni Bank database (http://www.lexgen.com) of ES cell clones with retrovirus insertions, we identified a clone containing a retroviral integration in the first intron of mouse *SIP* (Figure 1A). A polymerase chain reaction (PCR) was established for distinguishing the intact and targeted *SIP* genes (Figure 1B). Using these ES cells, we obtained mice carrying the disrupted *SIP* gene and observed that homozygous *SIP* knockout mice are born with normal Mendelian ratios, indicating that *SIP* is not an essential gene. $SIP^{-/-}$ mice grow normally and do not develop spontaneous malignancies or other diseases. Mouse embryonic fibroblasts (MEFs) were derived from day 14.5 (E14.5) $SIP^{+/+}$, $SIP^{+/-}$, and $SIP^{-/-}$ embryos and analyzed by immunoblotting to determine the levels of SIP expression. Whole-cell lysates from MEFs showed detectable amounts of SIP protein in $SIP^{+/+}$ and $SIP^{+/-}$ mice, but not in $SIP^{-/-}$ mice. SIP protein levels were lower in $SIP^{+/-}$ than in $SIP^{+/+}$ mice, indicating a dose-dependent expression of both *SIP* alleles (Figure 1C). DNA and RNA isolated from MEFs were analyzed by Southern and northern blotting, respectively, with ^{32}P-labeled *mSIP* cDNA probes, confirming disruption of the *SIP* gene and loss of *SIP* mRNA expression in $SIP^{-/-}$ cells (Figures 1D and 1E).

Smaller Thymus and Spleen Size in SIP-Deficient Mice

$SIP^{-/-}$ mice were fertile and grew normally during 18 months of observation. However, we noticed that $SIP^{-/-}$ mice have smaller thymus and spleen size than wild-type mice (Figure 2A). Indeed, 4-week-old $SIP^{-/-}$ mice have thymi and spleens that have ~50% the cellularity of organs from wild-type littermates (Figure 2B). This difference in cellularity was not as prominent in 8-month-old $SIP^{-/-}$ mice, which have ~85% of the cells in the thymus and spleen in comparison to wild-type littermates. This phenotype is similar to that of mice expressing stabilized β-catenin in the thymus (Gounari et al., 2001). Histological analysis of the thymus glands of $SIP^{-/-}$ mice showed slightly smaller medullas compared to $SIP^{+/+}$ mice (Figure 2C). Also, in the spleen, the size of the T and B areas were reduced in $SIP^{-/-}$ mice (Figures 2D–2F), although the splenic structure

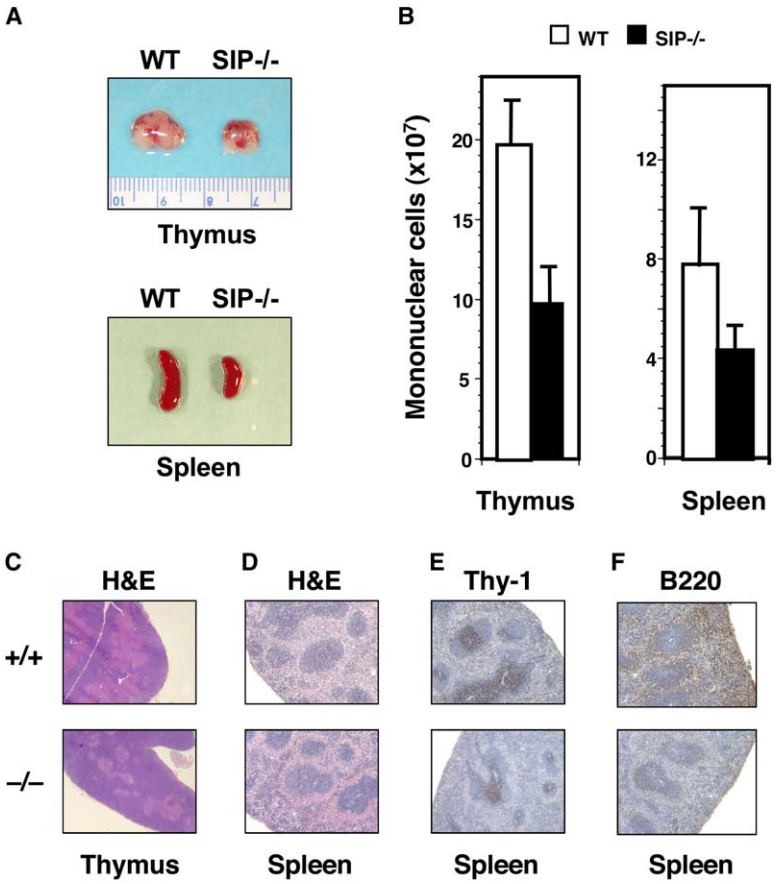

Figure 2. Size and Cellularity of Thymus and Spleen Are Reduced in SIP-Deficient Mice

(A) Photographs of thymi and spleens from 4-week-old wild-type and *SIP*$^{-/-}$ mice.

(B) Total cell numbers contained in whole thymi or spleens from 4-week-old wild-type (n = 8) and *SIP*$^{-/-}$ mice (n = 7) are shown.

(C–F) *SIP*$^{+/+}$ and *SIP*$^{-/-}$ mice at 4 weeks of age were sacrificed, and histological analyses were performed. Representative examples are shown: (C) H&E analysis of thymus, (D) H&E analysis of spleens, (E) anti-Thy-1 staining of spleens, and (F) anti-B220 staining of spleens.

appeared normal (Figure 2B), thus suggesting a role for SIP in B and T lymphocytes homeostasis.

Pre-TCR Checkpoint Is Impaired in SIP-Deficient Thymocytes

Thymocytes develop from a double-negative (DN) stage lacking expression of CD4 and CD8 to a double-positive stage (DP), and they then mature to single-positive (SP) T cells expressing either CD4 or CD8 and displaying surface αβTCR expression (Figure 3A). The DN stage can be further divided into four successive developmental stages identified by the differential expression of CD44 and CD25 on the surface of DN thymocytes: DN1 (CD44^{+}CD25^{+}), DN2 (CD44^{+}CD25^{-}), DN3 (CD44^{-}CD25^{+}), and DN4 (CD44^{-}CD25^{-}). *TCRβ* gene rearrangements occur at the DN3 stage, resulting in the expression of a pre-TCR (receptor complexes of TCRβ, pTα, and CD3 chains lacking the TCR α-chain). The signals provided by the pre-TCR together with other signals provided by the thymic microenvironment, such as Wnt signaling, support the transition of DN cells to the DP stage. Thymocytes without pre-TCR signaling undergo cell-cycle arrest and apoptosis, defining the pre-TCR checkpoint (Wu and Strasser, 2001). Furthermore, p53 plays an important role in the pre-TCR checkpoint (Bogue et al., 1996; Guidos et al., 1996; Haks et al., 1999; Jiang et al., 1996).

To examine whether SIP-dependent β-catenin degradation is required for the pre-TCR checkpoint, we performed flow-cytometry analyses of thymocytes from 4-week-old wild-type and *SIP*$^{-/-}$ mice. Whereas both *SIP*$^{-/-}$ and wild-type mice have similar percentages of DP and CD4 and CD8 single-positive T cell populations (Figure 3B), the analysis of the DN population showed an accumulation of the DN3 population in *SIP*$^{-/-}$ mice (Figure 3B). Also, among the thymocytes that did manage to progress to the DN4 stage in *SIP*$^{-/-}$ mice, intracellular TCRβ expression was reduced, compared to wild-type mice (Figure 3C), similar to observations previously made for mice in which stabilized β-catenin was expressed in thymus (Gounari et al., 2001).

To further confirm that *SIP*$^{-/-}$ thymocytes are able to develop from DN3 to DN4 stage in the absence of *TCRβ* gene rearrangement, we measured catalytic activity of recombinase in *SIP*$^{-/-}$ thymocytes. Recombination-activating genes *RAG1* and *RAG2* are essential for the first step of V(D)J recombination in *TCR* gene rearrangement. Mice lacking either of these genes are unable to undergo V(D)J recombination, causing a complete block of thymocyte differentiation at the pre-TCR checkpoint (Mombaerts et al., 1992; Shinkai et al., 1992). To measure recombinase activity, we used a retroviral vector that contains the 12- and 23-recombination signal sequences (RSS), separated by a reverse EGFP cDNA relative to 5′LTR (Figure 3D). The retroviral vector integrates into the host genome, whereas the LTR induces bicistronic transcripts that allow for the simultaneous assessment of recombination resulting in inversion of the GFP cassette and GFP expression (Liang et al., 2002). As shown in Figure 3E, recombinase activity

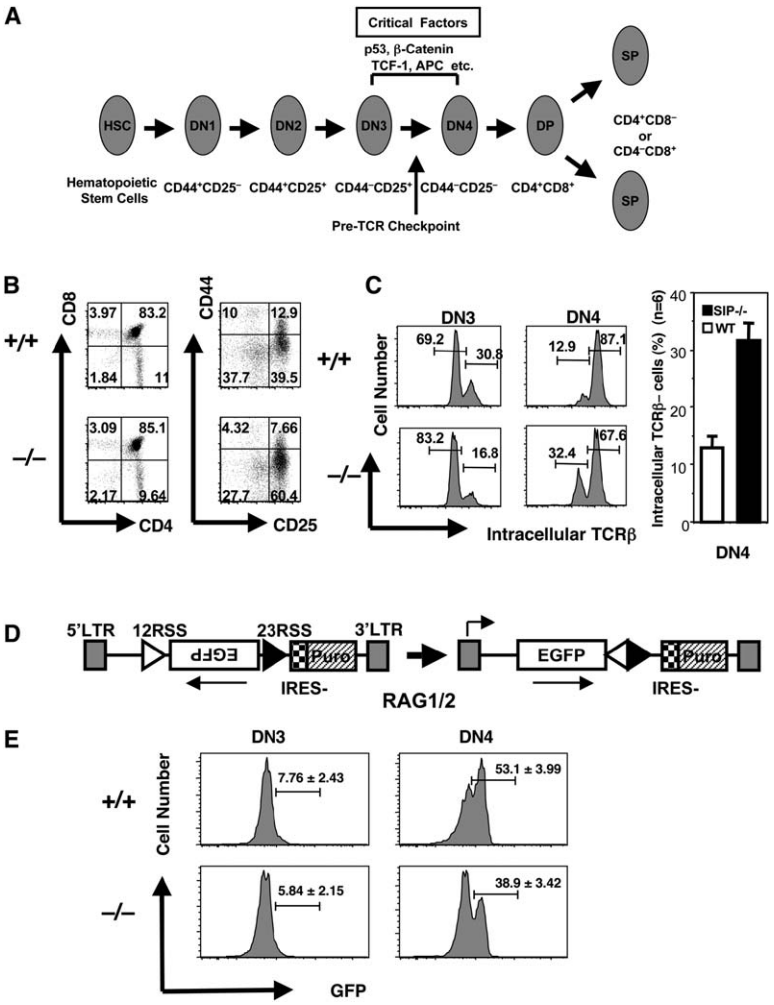

Figure 3. Impaired pre-TCR Checkpoint and Increased Apoptosis in SIP-Deficient Thymocytes

(A) T cell differentiation in the thymus. Representative receptors and transcription factors that are critical for the different transition stages are indicated. DN denotes double-negative, DP denotes double-positive, and SP denotes single-positive T cells.

(B) *SIP*$^{+/+}$ and *SIP*$^{-/-}$ thymocytes were stained with antibodies to CD4, CD8, TCR$\gamma\delta$, DX5, B220 (lineage marker, Lin), CD25, and CD44. At left: CD4 and CD8 expression of the total thymocyte population. At right: CD44 and CD25 expression (gated in Lin- cells). The percentages of cells in each quadrant are shown. Data are representative of six experiments.

(C) Intracellular TCRβ expression was analyzed in DN3 (CD44^{-}CD25^{+}) and DN4 (CD44^{-}CD25^{-}) thymocytes from *SIP*$^{+/+}$ and *SIP*$^{-/-}$ mice. Left panel shows representative data (n = 6). The right panel shows mean ± standard error of the mean (SEM) for six experiments, indicating percentage of DN4 thymocytes without TCRβ intracellular staining. The difference in percentage of TCRβ-negative DN4 cells is statistically significant (unpaired t test, $p < 0.0009$).

(D) Schematic representation of the retroviral 12/23 rEGFP vector for functional analysis of RAG recombinase activity in thymocytes. The construct contains a reverse EGFP reporter (rEGFP) oriented between 12 (open triangle) and 23 (closed triangle) RSS (Recombination Signal Sequence). The rEGFP reporter is inverted to the sense orientation by RAG recombinase activity (Liang et al., 2002).

(E) Thymocytes were infected with the retroviral 12/23 rEGFP vector for 48 hr. Cells were then stained with antibodies to Lin, CD25, and CD44. GFP-positive cells were analyzed in DN3 and DN4 thymocytes from *SIP*$^{+/+}$ and *SIP*$^{-/-}$ mice. Representative data shows DN3 and DN4 thymocytes, showing GFP fluorescence. Numbers show mean ± SEM percentage of GFP-positive thymocytes for six experiments. The difference in percentage of GFP-positive DN4 cells is statistically significant (unpaired t test, $p < 0.0009$).

was significantly reduced in *SIP*$^{-/-}$ DN4 cells compared with wild-type cells, but not in DN3 cells. Thus, the absence of SIP allows thymocytes to progress to the DN4 stage despite absence of recombinase activity, indicating that these SIP-deficient cells defy a checkpoint in thymic development, akin to observations from mice with constitutive expression of β-catenin in thymocytes (Gounari et al., 2001).

Accumulation of β-catenin Protein and Increased Apoptosis in SIP-Deficient Thymocytes

To confirm that SIP deficiency results in elevated β-catenin expression in the developing thymus, we isolated DN cells by cell sorting and compared β-catenin levels in wild-type and mutant mice. DN thymocytes were fractionated into Triton X-100-soluble and -insoluble fractions to distinguish cytosolic versus nuclear β-catenin (Sadot et al., 2000, Sadot et al., 2001). As shown in Figure 4A, the level of β-catenin in *SIP*$^{-/-}$ DN cells was remarkably increased in both the Triton X-100-soluble and -insoluble fractions compared to wild-type thymocytes. To analyze the β-catenin levels in thymocytes more quantitatively, we evaluated intracellular β-catenin immunostaining by flow cytometry and combined it with surface staining for CD4, CD8, CD25, and CD44 antigens (Figure 4B). Increased accumulation of β-catenin protein was observed in *SIP*$^{-/-}$ DN3 cells compared to wild-type DN3 cells, and to a lesser extent in DN4 thymocytes.

Altogether, these results suggest that SIP-deficient thymocytes reach the DN3 stage of thymic development, then either fail to complete differentiation or die. Because *SIP*$^{-/-}$ mice showed reduced thymic cellularity compared to wild-type mice, we hypothesized that immature *SIP*$^{-/-}$ thymocytes undergo apoptosis after disobeying the pre-TCR checkpoint. To examine this possibility, we analyzed the survival of thymocytes in culture by Annexin V staining. Apoptotic cells were increased among the DN4 (1.4-fold) and the DP (1.8-fold) populations in *SIP*$^{-/-}$ thymocytes (Figure 4C), suggesting that SIP deficiency increases apoptosis of developing thymocytes at these stages of development in a manner similar to what has been reported in mice with constitutive expression of β-catenin in thymocytes (Gounari et al., 2001). In contrast, the frequency of apoptotic cells

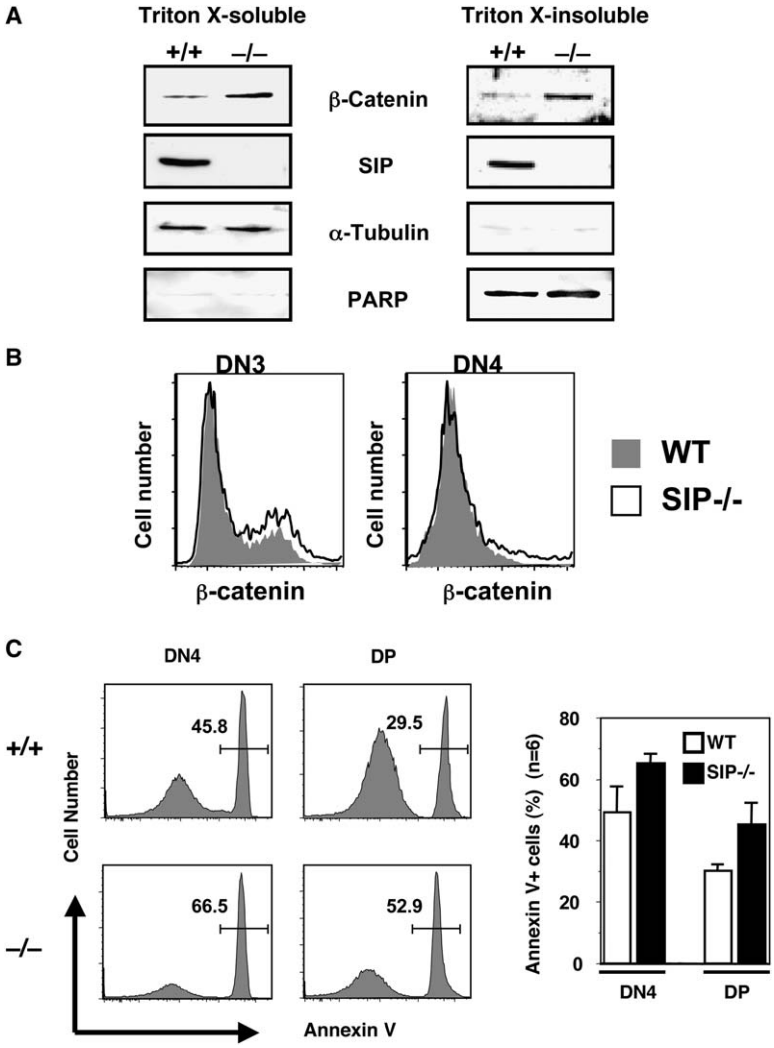

Figure 4. Increased Protein β-Catenin Levels and Apoptosis in SIP-Deficient Thymocytes

(A) $SIP^{+/+}$ and $SIP^{-/-}$ thymocytes (1×10^9) were stained with antibodies to CD4, CD8, TCRγδ, DX5, and B220 (Lin). Lin-negative thymocytes were purified by cell sorting, and equal amounts of Triton X-100-soluble (cytosolic) and Triton X-100-insoluble (nuclear fractions) material from DN thymocytes (20 μg/lane) were analyzed by immunoblotting with anti-β-catenin and anti-SIP antibodies. The membranes were reprobed with antibodies to α-tubulin (cytosolic markers) and PARP (nuclear markers).

(B) Thymocytes were stained with antibodies to Lin, CD44, and CD25. Cells were then permeabilized and stained with anti-β-catenin-fluorescein isothiocyanate antibody. Intracellular β-catenin expression was analyzed in DN3 and DN4 thymocytes from $SIP^{+/+}$ and $SIP^{-/-}$ mice. Data are representative of six independent experiments.

(C) Thymocytes were cultured for 24 hr and then stained with antibodies to Lin (CD4, CD8, TCRγδ, DX5, and B220), CD44, CD25, and Annexin V. The left panel shows representative data for Annexin V staining results for DN4 and DP thymocytes. The right panel shows mean ± SEM for % Annexin-V-positive thymocytes at the DN4 and DP stages (n = 6). The increased percentage of Annexin-V-positive for $SIP^{-/-}$ thymocytes at the DN4 ($p < 0.007$) and DP ($p < 0.004$) stage is statistically significant (unpaired t test).

was not increased within the DN3 population (data not shown). These data suggest that by disobeying the pre-TCR checkpoint, $SIP^{-/-}$ thymocytes inappropriately proceed from the DN3 to DN4 and DP stage, resulting in reduced survival.

SIP-Deficient Cells Show Impaired β-Catenin Degradation and Defective G1 Cell-Cycle Checkpoint After γ Irradiation and UV Irradiation

p53 plays an important role in the G1 cell-cycle checkpoint induced by ionizing radiation (Kastan et al., 1992; Wahl and Carr, 2001). MEFs provide an ideal cell model system for studying p53-mediated G1 arrest (Attardi et al., 2004). For example, wild-type MEFs treated with γ irradiation undergo p53-dependent G1 arrest, whereas $p53^{-/-}$ MEFs fail to arrest (Kastan et al., 1992). For exploring the role of SIP in the G1 checkpoint induced by DNA damage, early-passage MEFs from $SIP^{+/+}$ and $SIP^{-/-}$ embryos were subjected to γ irradiation (20 Gy), and the percentage of cells entering S phase was determined 24 hr later (Figure 5A). Prior to γ irradiation, $SIP^{-/-}$ MEFs entered S phase more rapidly than wild-type MEFs upon serum addition, but less than $p53^{-/-}$ MEFs. After 20 Gy γ irradiation, S phase entry by wild-type MEFs was markedly suppressed. In contrast, $p53^{-/-}$ MEFs underwent S phase progression regardless of γ irradiation. $SIP^{-/-}$ cells displayed a phenotype intermediate between wild-type and $p53^{-/-}$ MEFs (Figure 5A). This phenotype of $SIP^{-/-}$ cells is quite similar to MEFs from $p21^{-/-}$ mice (Deng et al., 1995). These results suggest that SIP is partially required for the G1-phase checkpoint induced by γ irradiation.

Next, we examined levels of endogenous β-catenin protein by immunoblotting. As expected, γ irradiation triggered a decline in β-catenin levels in $SIP^{+/+}$ MEFs. In contrast, $SIP^{-/-}$ and $p53^{-/-}$ MEFs failed to downregulate β-catenin in response to γ irradiation (Figure 5B).

In addition to the G1 checkpoint, p53 is also known to control the mitotic spindle checkpoint (Cross et al., 1995). To examine whether SIP also has a role in mitotic spindle-checkpoint regulation, we compared the induction of polyploidy by nocodazole in wild-type, $SIP^{-/-}$, and $p53^{-/-}$ MEFs. Nocodazole-treated $SIP^{+/+}$ MEFs arrested with 4N DNA content (Figure 5C). In contrast, $p53^{-/-}$ MEFs failed to arrest, proceeding through cell cycle to become polyploid. Cells lacking SIP showed an intact mitotic checkpoint, thus indicating that SIP is not required for the mitotic spindle checkpoint.

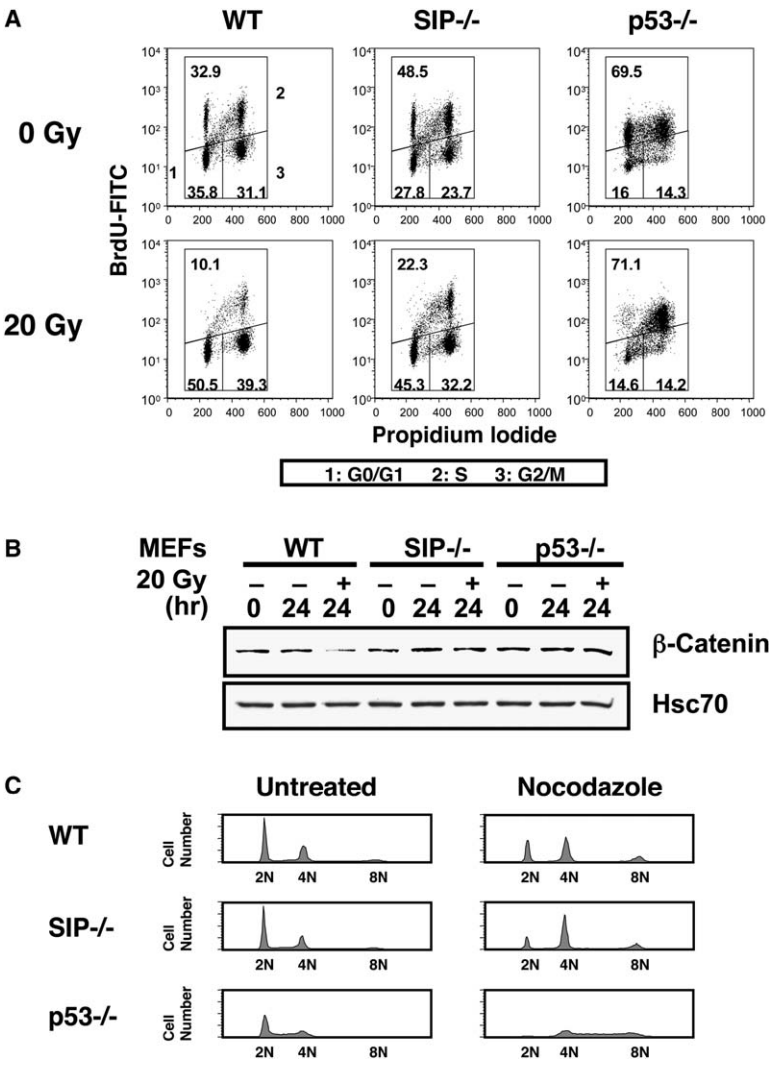

Figure 5. SIP Deficiency Impairs β-Catenin Degradation and G1 Cell-Cycle Arrest after γ Irradiation

(A) Serum-starved MEFs were released into complete media containing BrdU (65 μM) with no treatment or 20 Gy γ irradiation. After 24 hr, cells were harvested and analyzed by flow cytometry. Boxes labeled 1, 2, and 3 indicate G0/G1, S, and G2/M phase cells, respectively. The percentage of cells in each phase of the cell cycle is shown in each diagram.

(B) Serum-starved MEFs (96 hr) derived from wild-type (WT), $SIP^{-/-}$, and $p53^{-/-}$ mice were released into complete media with no treatment or 20 Gy γ irradiation. After 24 hr, cytosolic fractions were analyzed by immunoblotting. All the membranes were reprobed with goat anti-Hsc70 antibody as a control.

(C) Asynchronous wild-type (WT), $SIP^{-/-}$, and $p53^{-/-}$ MEFs were incubated in the absence or presence of 125 ng/ml nocodazole for 24 hr. Cells were harvested and their DNA contents were determined by FACS after DNA staining with propidium iodide. DNA-content FACS histograms are shown, as are the positions of peaks for cells with 2N, 4N, and 8N DNA content. Each of these experiments was repeated three times with similar results.

Having observed that SIP is required for β-catenin degradation and G1 arrest following γ irradiation, we next examined the effects of SIP deficiency in response to UV irradiation, which we have described induces Siah1 expression and β-catenin degradation (Iwai et al., 2004; Matsuzawa et al., 1998). For these experiments, early-passage MEFs were prepared from $SIP^{+/+}$, and $SIP^{-/-}$ embryos and subjected to UV irradiation, and then the number of viable cells was counted at various times thereafter. Low-dose UV irradiation (10–20 J/m^2) induced proliferation arrest of wild-type (WT) MEFs without inducing substantial apoptosis, whereas $SIP^{-/-}$ MEFs continued to proliferate at nearly normal rates (data not shown). UV irradiation triggered a decline in endogenous β-catenin protein levels in MEFs from $SIP^{+/+}$ (Figure 6A) and $SIP^{+/-}$ mice (data not shown). In contrast, $SIP^{-/-}$ MEFs failed to downregulate β-catenin (Figure 6A). Similarly, β-catenin levels were not reduced in UV-irradiated $p53^{-/-}$ MEF cells, consistent with the hypothesis that p53 and SIP operate in the same β-catenin degradation pathway. A similar result was obtained with splenocytes from $SIP^{-/-}$ mice (Figure 6B). Interestingly, the basal levels of endogeneous β-catenin protein were higher in $SIP^{-/-}$ lymphocytes than in $SIP^{+/+}$ and $SIP^{+/-}$ cells, further supporting a role for SIP in regulating endogenous β-catenin expression.

SIP-Deficient MEFs Show Enhanced Proliferative Properties

Using early-passage MEFs from $SIP^{+/+}$, $SIP^{+/-}$, and $SIP^{-/-}$ embryos, we compared the proliferative properties of cells with different levels of SIP. At low passage (e.g., passage 3), growth rates of MEFs from $SIP^{-/-}$ embryos were higher than MEFs from $SIP^{+/+}$ and $SIP^{+/-}$ embryos. All MEFs showed contact inhibition, but the monolayers formed by $SIP^{-/-}$ MEFs were more crowded than those formed by $SIP^{+/+}$ and $SIP^{+/-}$. In addition, the saturation densities of $SIP^{-/-}$ MEFs were significantly higher than those of wild-type and $SIP^{+/-}$ MEFs (Figure 7A). At later passage (e.g., passage 7), proliferation of $SIP^{+/+}$ and $SIP^{+/-}$ MEFs was significantly reduced, whereas the proliferation of $SIP^{-/-}$ MEFs remained robust (Figure 7A).

Activation of Tcf/LEF-family transcription factors by β-catenin is known to induce expression of *cyclin D1*, *c-myc*, and other genes important for cell proliferation (He et al., 1998; Tetsu and McCormick, 1999). To further examine the role of SIP in cell-cycle progression, we

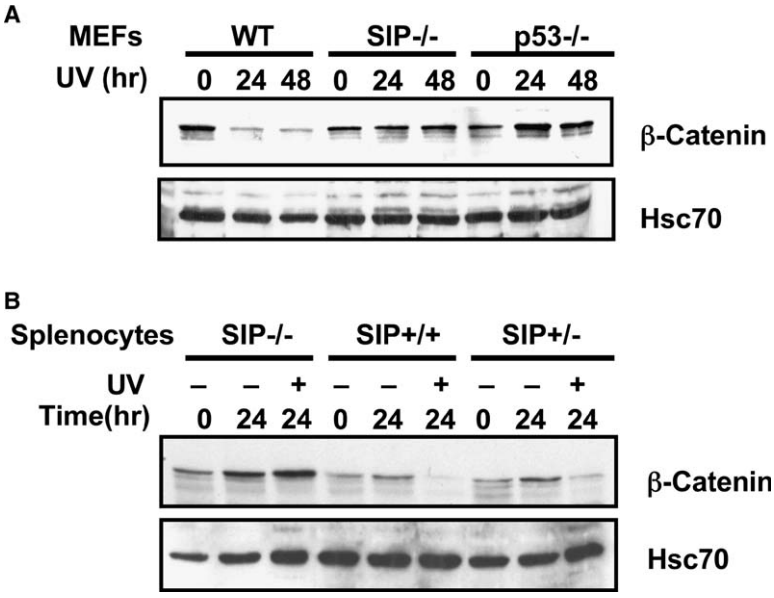

Figure 6. SIP Deficiency Impairs UV-Induced β-Catenin Degradation and Cell-Cycle Arrest

(A) MEFs derived from wild-type (WT), $SIP^{-/-}$, and $p53^{-/-}$ mice were cultured for 24 hr prior exposure to 20 J/m^2 UV irradiation. After 24 or 48 hr, cytosolic fractions were analyzed by immunoblotting. The membrane was reprobed with goat anti-Hsc70 antibody as a control.

(B) Splenocytes derived from $SIP^{-/-}$, $SIP^{+/+}$, and $SIP^{+/-}$ mice were cultured for 24 hr with (+) or without (–) prior exposure to 10 J/m^2 UV irradiation. Cytosolic fractions were prepared from control or UV-irradiated cells (after 24 hr) and aliquots (20 μg) were analyzed by immunoblotting, with antibodies specific for β-catenin. The membrane was reprobed with goat anti-Hsc70 antibody as a control.

analyzed the expression of β-catenin target genes by using serum-starved wild-type, $SIP^{-/-}$, and $p53^{-/-}$ MEFs. After serum starvation, cells were cultured in complete media and harvested 3 hr and 9 hr later, respectively, and the levels of induction of Cyclin D1 and c-Myc were compared. As shown in Figure 7B, $SIP^{-/-}$ MEFs showed faster and higher induction of Cyclin D1 and c-Myc protein expression than wild-type MEFs, similar to what is observed in $p53^{-/-}$ MEFs. These data are consistent with previous reports describing a role for β-catenin as a transcriptional regulator of *cyclin D1* and *c-myc* genes (He et al., 1998; Tetsu and McCormick, 1999).

Discussion

In this study, we showed that SIP-deficient embryonic fibroblasts have a faster growth rate and express *cyclin D1* and *c-myc* at increased levels in comparison to wild-type MEFs. We also show that these cells are partially

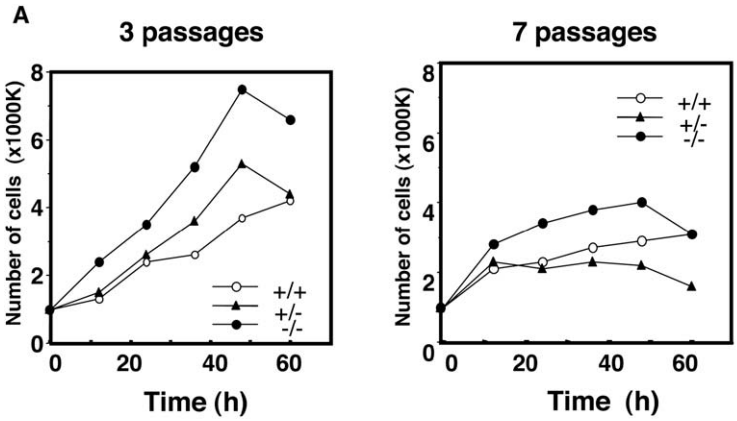

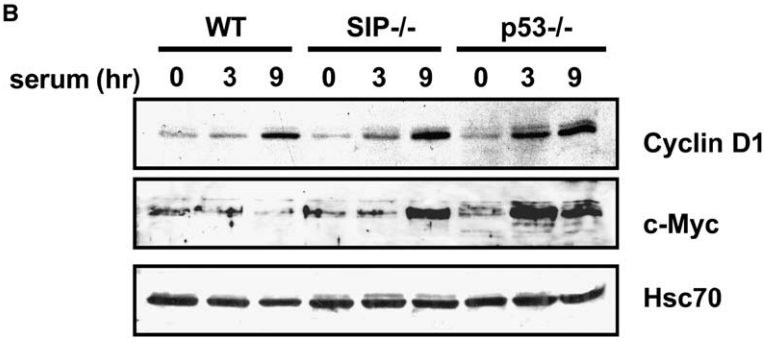

Figure 7. SIP Deficiency Enhances Proliferation of MEFs

(A) Growth analysis of MEFs were performed at passage 3 (early passage) and passage 7 (late passage). Cells (5 × 10^6) from $SIP^{+/+}$, $SIP^{+/-}$, and $SIP^{-/-}$ mice (as indicated in figures) were seeded into 60 mm dishes, and cell numbers were counted at various times. Representative data from three independents experiments are shown.

(B) Serum-starved MEFs (96 hr) derived from wild-type (WT), $SIP^{-/-}$, and $p53^{-/-}$ mice were released into complete media. At 3 and 9 hr after release, whole-cell lysates of MEFs were subjected to SDS-PAGE immunoblotting with anti-Cyclin D1, anti-c-Myc and anti-Hsc70 antibodies.

deficient in their ability to arrest in G1 following DNA damage. SIP-deficiency also inhibits β-catenin downregulation induced by p53-activating stimuli. $p21^{waf-1}$ is a well-known G1 cell-cycle inhibitor induced by p53. However, $p21^{-/-}$ MEFs show only a partial defect in the G1 cell-cycle checkpoint in response to DNA damage, suggesting the existence of other p53-dependent G1 checkpoint pathways. Taken together with previous results, these observations demonstrate that SIP is required for this alternative p53-dependent G1 checkpoint. Although a G1-checkpoint failure may lead to cancer, it is interesting to note that neither $p21^{-/-}$ nor $SIP^{-/-}$ mice develop spontaneous tumors, suggesting that combined deficiency of p21 and SIP may be necessary for tumorigenesis.

Furthermore, we found that $SIP^{-/-}$ mice have smaller thymus glands and spleens than wild-type mice as a result of reduced lymphocyte cellularity. Recently, β-catenin has been implicated in T cell development. Indeed, deletion of β-catenin, Tcf-1, or adenomatous poliposis coli (APC) in the thymus impairs the transition from DN3 to DN4 stage (Gounari et al., 2005; Ioannidis et al., 2001; Xu et al., 2003). In contrast, conditional stabilization of active β-catenin in the thymus results in escape from the pre-TCR checkpoint and promotes thymocyte transition from the DN3 to DN4 and then to the DP stage in the absence of TCRβ selection (Gounari et al., 2001). However, while promoting differentiation, expression of active β-catenin in thymocytes results in reduced cellularity of the thymus, apparently as a result of apoptosis induction (Gounari et al., 2001). SIP deficiency produces a remarkably similar phenotype as enforced expression of β-catenin protein in DN cells, further underlining the essential role of β-catenin in thymocyte development. Indeed, DN3 $SIP^{-/-}$ thymocytes appeared to transit to the DN4 stage in the absence of pre-TCR signaling, given that $SIP^{-/-}$ DN4 cells contained abnormally low levels of TCRβ. Also, like β-catenin-overexpressing mice, the thymus glands of $SIP^{-/-}$ mice have reduced cellularity, and thymocytes undergo increased apoptosis in culture.

The phenotype of $SIP^{-/-}$ mice is relatively modest compared with mice in which stabilized β-catenin was expressed or *APC* gene was disrupted in thymocytes (Gounari et al., 2001, Gounari et al., 2005). As shown in Figures 4A and 4B, levels of β-catenin in $SIP^{-/-}$ DN thymocytes were 3–4 times higher than in wild-type mice. However, β-catenin-overexpressing mice and $APC^{-/-}$ mice show a huge accumulation of β-catenin in thymocytes (Gounari et al., 2001, Gounari et al., 2005), suggesting that the severity of the phenotype is determined by the magnitude of β-catenin accumulation. We would propose that the degree of β-catenin accumulation seen in our $SIP^{-/-}$ mice is probably more physiological than the amounts observed in mice with stabilized β-catenin.

In addition to β-catenin, p53 is also implicated in the control of the pre-TCR checkpoint. Loss of p53 in pre-TCR-deficient thymocytes promotes their survival and differentiation in the absence of *TCR* gene rearrangements (Bogue et al., 1996; Guidos et al., 1996; Haks et al., 1999; Jiang et al., 1996). The fact that p53 and SIP loss phenocopy each other in this regard suggests a functional connection between p53 and β-catenin degradation in the pre-TCR checkpoint, consistent with prior data showing that p53 induces Siah1 expression (Fiucci et al., 2004). It has been hypothesized that double-strand-DNA breaks during V(D)J recombination trigger the p53 pathway to delay cell-cycle progression at the G1 checkpoint (Nelson and Kastan, 1994). However, suppression of recombinase activity was observed in $SIP^{-/-}$ DN cells, similar to observations made for mice with stabilized β-catenin and $APC^{-/-}$ mice (Gounari et al., 2001, Gounari et al., 2005). These observations may rather support a hypothesis that cell-cycle arrest is required to initiate *TCR* gene rearrangements, with $SIP^{-/-}$ and $APC^{-/-}$ thymocytes failing to arrest and thus differentiating without *TCR* gene rearrangements. Regardless of the explanation, our data show that SIP is required to prevent maturation of thymocytes in the absence of *TCR* gene rearrangements, which is a phenotype observed in p53-null and APC-null mice, consistent with prior data linking p53, APC, and SIP into a pathway controlling β-catenin degradation (Gounari et al., 2001, Gounari, et al., 2005).

$Siah1a^{-/-}$ mice also have reduced cellularity (30%–50% that of normal mice) of lymphoid organs, including thymus, spleen, and lymph nodes, suggesting a role for Siah1 in lymphoid development (Frew et al., 2004). Siah-family proteins bind ubiquitin-conjugating enzymes (UBCs) via an N-terminal RING domain and target other proteins for degradation. Twenty-three potential target proteins of Siah-mediated degradation have been reported, including DCC, a putative tumor-suppressor protein possibly involved in colon cancers (Hu et al., 1997); N-CoR, a transcriptional corepressor that regulates nuclear steroid hormone and retinoid receptors (Zhang et al., 1998); PHD1/3, a family of prolyl-hydroxylases (Nakayama et al., 2004); and the proto-oncogene c-Myb (Tanikawa et al., 2000). Although there is no direct evidence that SIP is involved in Siah-induced degradation of these proteins, it has been reported that c-Myb is required for development of thymocytes at the DN3 stage, as well as for survival of DP cells and for differentiation of SP cells (Bender et al., 2004; Lieu et al., 2004). These observations thus suggest that SIP may control stability of other proteins in addition to β-catenin. Thus, further studies should address the role of SIP in controlling the stability of c-Myb and other proteins that are known targets of Siah1.

Experimental Procedures

Generation of SIP-Deficient Mice and Genotyping

Searching the Omni Bank database (http://www.lexgen.com) for ES cell clones with retrovirus insertions in the *SIP* gene, we found a clone in which the integration site for the retrovirus was located in the first intron of mouse *SIP* gene. The position of retrovirus insertion was determined by Southern blotting with probes derived from exon 2 of mouse *SIP* gene, which was amplified by PCR methods. Genomic DNA was isolated from MEFs of wild-type and *SIP*-deficient littermate mice. A total of 10 μg of DNA was digested with XbaI and size fractionated in agarose-gel electrophoresis, followed by transfer to Hybond N+ nylon membranes. Membranes were incubated with random primed ^{32}P-labeled mouse *SIP* cDNA probe in 10% dextran-sulfate, 1% SDS, and 1 M NaCl solution at 68ºC for overnight. Membranes were washed with 2× SSC, 0.1% SDS at room temperature, followed by 1× to 0.1× SSC at increased temperature. Autoradiography was performed overnight at −80ºC with Kodak AR film.

Cell Culture

Primary MEFs were derived from E14.5 embryos according to standard protocols (Chae et al., 2004). *p53*$^{-/-}$ MEFs were kindly provided by Dr. Inder M. Verma (The Salk Institute). Cells were cultured at 37ºC (5% CO_2) in high-glucose Dulbecco's modified Eagle's medium (DMEM, Irvine Scientific) with 10% fetal calf serum (FCS), 1 mM L-glutamine, and antibiotics (DMEM 10). For the experiments using serum-starved cells, asynchronous cells at 70% confluence were washed with phosphate-buffered saline, placed in DMEM containing 0.1% FCS (DMEM 0.1) for 96 hrs, and then trypsinized in growth medium before being subjected to γ irradiation. Cell were irradiated at 0 or 20 Gy and then cultured in DMEM 10.

Thymocyte Immunophenotyping

The following monoclonal antibodies (mAbs) for flow cytometry were obtained from BD Biosciences Pharmingen: anti-CD4, anti-CD8, anti-CD25, anti-CD44, anti-TCRβ(H57-597), anti-TCR$\gamma\delta$(GL3), anti-DX5, and anti-B220. These mAbs were directly coupled to fluorescein isothiocyanate (FITC), phycoerythrin, cyanine-dye-coupled peridinin chlorophyll protein (PerCP-Cy5.5), or allophycocyanin. Thymocytes were incubated with 2.4G2 (anti-CD16/32) to reduce the background. Cells were flow sorted with a FACSCanto (BD Biosciences Pharmingen), and data were analyzed with FlowJo software (Tree Star).

Intracellular-Thymocyte Staining

Thymocytes were labeled for cell-surface markers to define DN3 and DN4 stages. The cells were then fixed for 10 min in PBS with 2% paraformaldehyde at room temperatur, and incubated with anti-TCRβ or anti-β-catenin-FITC (14, BD Bioscience) in PBS with 3% FCS and 0.5% Saponin (Sigma). After washing with PBS with 3% FCS and 0.5% Saponin, cells were sorted and analyzed.

Apoptosis Analysis

Thymocytes were suspended at a density of 1×10^6/ml in RPMI 1640 medium with 10% FCS, 50 μM β-mercaptoethanol, and 1 mM L-glutamine and antibiotics. Cells were cultured at 37ºC (5% CO_2) for 24 hr and then stained for cell-surface markers to define the stage of differentiation. Apoptotic cells were identified by Annexin V-FITC staining (BioVision).

Histological Analysis

Tissues were dissected and fixed in zinc-buffered formalin (Z-fix, Anatech). Paraffin sections (0.5 μm) were prepared by standard procedures and stained with hematoxylin and eosin (H&E). For immunohistochemistry, paraffin sections were deparaffinized by standard procedures and then incubated with anti-Thy-1 antibody or anti-B220 antibody (BD-Biosciences). The sections were visualized with 3,3-Diaminobenzidine and counterstained with hematoxyline.

Cell-Cycle Analysis

Cells were pulse labeled with 10 μM BrdU (4 hr; Sigma) for asynchronous cells or with 65 μM (24 hr) for synchronized cells. Labeled cells were fixed in 70% ethanol and stored at −20ºC overnight. Cells were denatured by incubation with 2 N HCl and 0.5% Triton X-100 for 30 min at room temperature, followed by neutralization with 0.1 M Sodium Tetraborate (pH 8.5). Cells were subjected to dual-color staining with FITC-conjugated anti-BrdU mAb (BD Biosciences) and 5 μg/ml propidium iodide. Cell-cycle analyses were carried out with FACSort (Becton Dickinson) and FlowJo software (Tree Star).

Immunoblotting

Cells were lysed with RIPA buffer (50 mM Tris-HCl (pH 7.4), 150 mM NaCl, 1% NP-40, 0.5% Deoxycholic acid, 0.1% SDS). Equal amounts of cell lysates were subjected to immunoblot analysis with antibodies to Cyclin D1 (DCS-6, BD Biosciences), c-Myc (N-262, Santa Cruz), or Hsc70 (K-19, Santa Cruz). For distinguishing cytosolic and nuclear β-catenin, cells were suspended in 50 mM MES buffer (pH 6.8) containing 2.5 mM EGTA, 5 mM $MgCl_2$, and 0.5% Triton X-100 (Sadot et al., 2000). Cell extracts were then centrifuged at 12,000 × g for 5 min, and resulting Triton X-100-soluble (cytosolic) fractions and Triton-X-insoluble (nuclear) fractions were separated by SDS-PAGE (12% gels) and transferred to nitrocellulose membranes. Proteins were detected with anti-β-catenin monoclonal antibody (14, BD Biosciences), and blots were reprobed with antibodies to α-tubulin (TU-01, Zymed Laboratories) and PARP (C2-10, BD Biosciences).

Retroviral-Infection GFP Reporter Assay

The retroviral 12/23 rEGFP vector was kindly provided by Dr. Cortez (Mt. Sinai School of Medicine). The vector contains a reverse EGFP reporter (rEGFP) between 12 and 23 RSS. For retroviral infection, 293T cells at 60%–70% confluence were transfected with 5 μg pMD.G (encodes vesicular stomatitis G Protein), 8 μg pMD.OGP (encodes gag-pol), and 10 μg retroviral 12/23 rEGFP vector for 48 hr. Thymocytes from *SIP*$^{+/+}$ and *SIP*$^{-/-}$ mice were infected with retroviral supernatant containing 50 μM β-mercaptoethanol and 4 μg/ml polybrene (Sigma) at 1×10^6 cells/ml in 24-well plates. For increasing infection efficiency, plates were centrifuged with a swing-bucket rotor at 1400 × g, 30ºC for 60 min. After 48 hr infection at 37ºC/5% CO_2, cells were harvested and analyzed by flow cytometry.

Acknowledgments

We thank Y. Altman, R. Newlin, and S. Banares for technical assistance, Drs. S. Hedrick and R. Abraham for helpful discussions, and Drs P. Cortez and I. Verma for reagents. This work was supported by the National Institutes of Health (CA107403; CA69381; CA67329; DK067515; CA078419) and Department of Defense W81XWH-05-1-0007. T.F. was supported by funds from the Japan Foundation for Aging and Health and a research fellowship from the Uehara Memorial Foundation.

Received: August 12, 2005
Revised: November 21, 2005
Accepted: December 14, 2005
Published: January 17, 2006

References

Abraham, R.T. (2001). Cell cycle checkpoint signaling through the ATM and ATR kinases. Genes Dev. *15*, 2177–2196.

Attardi, L.D., de Vries, A., and Jacks, T. (2004). Activation of the p53-dependent G1 checkpoint response in mouse embryo fibroblasts depends on the specific DNA damage inducer. Oncogene *23*, 973–980.

Bender, T.P., Kremer, C.S., Kraus, M., Buch, T., and Rajewsky, K. (2004). Critical functions for c-Myb at three checkpoints during thymocyte development. Nat. Immunol. *5*, 721–729.

Bogue, M.A., Zhu, C., Aguilar-Cordova, E., Donehower, L.A., and Roth, D.B. (1996). p53 is required for both radiation-induced differentiation and rescue of V(D)J rearrangement in scid mouse thymocytes. Genes Dev. *10*, 553–565.

Borowski, C., Martin, C., Gounari, F., Haughn, L., Aifantis, I., Grassi, F., and von Boehmer, H. (2002). On the brink of becoming a T cell. Curr. Opin. Immunol. *14*, 200–206.

Brugarolas, J., Chandrasekaran, C., Gordon, J.I., Beach, D., Jacks, T., and Hannon, G.J. (1995). Radiation-induced cell cycle arrest compromised by p21 deficiency. Nature *377*, 552–557.

Chae, H.J., Kim, H.R., Xu, C., Bailly-Maitre, B., Krajewska, M., Krajewski, S., Banares, S., Cui, J., Digicaylioglu, M., Ke, N., et al. (2004). BI-1 regulates an apoptosis pathway linked to endoplasmic reticulum stress. Mol. Cell *15*, 355–366.

Cross, S.M., Sanchez, C.A., Morgan, C.A., Schimke, M.K., Ramel, S., Idzerda, R.L., Raskind, W.H., and Reid, B.J. (1995). A p53-dependent mouse spindle checkpoint. Science *267*, 1353–1356.

Deng, C., Zhang, P., Harper, J.W., Elledge, S.J., and Leder, P. (1995). Mice lacking $p21^{CIP1/WAF1}$ undergo normal development, but are defective in G1 checkpoint control. Cell *82*, 675–684.

El-Deiry, W.S., Tokino, T., Velculescu, V.E., Levy, D.B., Parsons, R., Trent, J.M., Lin, D., Mercer, W.E., Kinzler, K.W., and Vogelstein, B. (1993). WAF1, a potential mediator of p53 tumor suppression. Cell *75*, 817–825.

Filipek, A., and Wojda, U. (1996). p30, a novel protein target of mouse calcyclin (S100A6). Biochem. J. *320*, 585–587.

Filipek, A., and Kuznicki, J. (1998). Molecular cloning and expression of a mouse brain cDNA encoding a novel protein target of calcyclin. J. Neurochem. *70*, 1793–1798.

Fiucci, G., Beaucourt, S., Duflaut, D., Lespagnol, A., Stumptner-Cuvelette, P., Geant, A., Buchwalter, G., Tuynder, M., Susini, L., Lassalle, J.M., et al. (2004). Siah-1b is a direct transcriptional target of p53: Identification of the functional p53 responsive element in the siah-1b promoter. Proc. Natl. Acad. Sci. USA *101*, 3510–3515.

Frew, I.J., Sims, N.A., Quinn, J.M., Walkley, C.R., Purton, L.E., Bowtell, D.D., and Gillespie, M.T. (2004). Osteopenia in Siah1a mutant mice. J. Biol. Chem. *279*, 29583–29588.

Gounari, F., Aifantis, I., Khazaie, K., Hoeflinger, S., Harada, N., Taketo, M.M., and von Boehmer, H. (2001). Somatic activation of β-catenin bypasses pre-TCR signaling and TCR selection in thymocyte development. Nat. Immunol. *2*, 863–869.

Gounari, F., Chang, R., Cowan, J., Guo, Z., Dose, M., Gounaris, E., and Khazaie, K. (2005). Loss of adenomatous polyposis coli gene function disrupts thymic development. Nat. Immunol. *6*, 800–809.

Guidos, C.J., Williams, C.J., Grandal, I., Knowles, G., Huang, M.T., and Danska, J.S. (1996). V(D)J recombination activates a p53-dependent DNA damage checkpoint in scid lymphocyte precursors. Genes Dev. *10*, 2038–2054.

Haks, M.C., Krimpenfort, P., van den Brakel, J.H., and Kruisbeek, A.M. (1999). Pre-TCR signaling and inactivation of p53 induces crucial cell survival pathways in pre-T cells. Immunity *11*, 91–101.

Hall, P.A., and Lane, D.P. (1997). Tumour suppressors: A developing role for p53? Curr. Biol. *7*, R144–R147.

Harper, J.W., Adami, G.R., Wei, N., Keyomarsi, K., and Elledge, S.J. (1993). The p21 Cdk-interacting protein Cip1 is a potent inhibitor of G1 cyclin-dependent kinases. Cell *75*, 805–816.

Hart, M., Concordet, J.P., Lassot, I., Albert, I., del los Santos, R., Durand, H., Perret, C., Rubinfeld, B., Margottin, F., Benarous, R., and Polakis, P. (1999). The F-box protein β-TrCP associates with phosphorylated β-catenin and regulates its activity in the cell. Curr. Biol. *9*, 207–210.

Hartwell, L.H., and Kastan, M.B. (1994). Cell cycle control and cancer. Science *266*, 1821–1828.

He, T.C., Sparks, A.B., Rago, C., Hermeking, H., Zawel, L., da Costa, L.T., Morin, P.J., Vogelstein, B., and Kinzler, K.W. (1998). Identification of c-MYC as a target of the APC pathway. Science *281*, 1509–1512.

Hoffman, E.S., Passoni, L., Crompton, T., Leu, T.M., Schatz, D.G., Koff, A., Owen, M.J., and Hayday, A.C. (1996). Productive T-cell receptor β-chain gene rearrangement: Coincident regulation of cell cycle and clonality during development in vivo. Genes Dev. *10*, 948–962.

Hu, G., Zhang, S., Vidal, M., Baer, J.L., and Fearon, E.R. (1997). Mammalian homologs of seven in absentia regulate DCC via the ubiquitin-proteasome pathway. Genes Dev. *11*, 2701–2714.

Ioannidis, V., Beermann, F., Clevers, H., and Held, W. (2001). The β-catenin-TCF-1 pathway ensures $CD4^+CD8^+$ thymocyte survival. Nat. Immunol. *2*, 691–697.

Iwai, A., Marusawa, H., Matsuzawa, S., Fukushima, T., Hijikata, M., Reed, J.C., Shimotohno, K., and Chiba, T. (2004). Siah-1L, a novel transcript variant belonging to the human Siah family of proteins, regulates β-catenin activity in a p53-dependent manner. Oncogene *23*, 7593–7600.

Jiang, D., Lenardo, M.J., and Zuniga-Pflucker, J.C. (1996). p53 prevents maturation to the $CD4^+CD8^+$ stage of thymocyte differentiation in the absence of T cell receptor rearrangement. J. Exp. Med. *183*, 1923–1928.

Kastan, M.B., Zhan, Q., el-Deiry, W.S., Carrier, F., Jacks, T., Walsh, W.V., Plunkett, B.S., Vogelstein, B., and Fornace, A.J., Jr. (1992). A mammalian cell cycle checkpoint pathway utilizing p53 and GADD45 is defective in ataxia-telangiectasia. Cell *71*, 587–597.

Kitagawa, K., Skowyra, D., Elledge, S.J., Harper, J.W., and Hieter, P. (1999a). SGT1 encodes an essential component of the yeast kinetochore assembly pathway and a novel subunit of the SCF ubiquitin ligase complex. Mol. Cell *4*, 21–33.

Kitagawa, M., Hatakeyama, S., Shirane, M., Matsumoto, M., Ishida, N., Hattori, K., Nakamichi, I., Kikuchi, A., and Nakayama, K. (1999b). An F-box protein, FWD1, mediates ubiquitin-dependent proteolysis of β-catenin. EMBO J. *18*, 2401–2410.

Latres, E., Chiaur, D.S., and Pagano, M. (1999). The human F box protein β-Trcp associates with the Cul1/Skp1 complex and regulates the stability of β-catenin. Oncogene *18*, 849–854.

Liang, H.E., Hsu, L.Y., Cado, D., Cowell, L.G., Kelsoe, G., and Schlissel, M.S. (2002). The "dispensable" portion of RAG2 is necessary for efficient V-to-DJ rearrangement during B and T cell development. Immunity *17*, 639–651.

Lieu, Y.K., Kumar, A., Pajerowski, A.G., Rogers, T.J., and Reddy, E.P. (2004). Requirement of c-myb in T cell development and in mature T cell function. Proc. Natl. Acad. Sci. USA *101*, 14853–14858.

Liu, J., Stevens, J., Hu, Y., Neufeld, K.L., White, R., and Matsunami, N. (2001). Siah-1 mediates a novel β-catenin degradation pathway linking p53 to the adenomatous polyposis coli protein. Mol. Cell *7*, 927–936.

Matsuzawa, S., and Reed, J.C. (2001). Siah-1, SIP, and Ebi collaborate in a novel pathway for β-catenin degradation linked to p53 responses. Mol. Cell *7*, 915–926.

Matsuzawa, S., Li, C., Ni, C.Z., Takayama, S., Reed, J.C., and Ely, K.R. (2003). Structural analysis of Siah1 and its interactions with Siah-interacting protein (SIP). J. Biol. Chem. *278*, 1837–1840.

Matsuzawa, S., Takayama, S., Froesch, B.A., Zapata, J.M., and Reed, J.C. (1998). p53-inducible human homologue of Drosophila seven in absentia (Siah) inhibits cell growth: Suppression by BAG-1. EMBO J. *17*, 2736–2747.

Mombaerts, P., Iacomini, J., Johnson, R.S., Herrup, K., Tonegawa, S., and Papaioannou, V.E. (1992). RAG-1-deficient mice have no mature B and T lymphocytes. Cell *68*, 869–877.

Mulroy, T., Xu, Y., and Sen, J.M. (2003). β-catenin expression enhances generation of mature thymocytes. Int. Immunol. *15*, 1485–1494.

Nakayama, K., Frew, I.J., Hagensen, M., Skals, M., Habelhah, H., Bhoumik, A., Kadoya, T., Erdjument-Bromage, H., Tempst, P., Frappell, P.B., et al. (2004). Siah2 regulates stability of prolyl-hydroxylases, controls HIF1α abundance, and modulates physiological responses to hypoxia. Cell *117*, 941–952.

Nelson, W.G., and Kastan, M.B. (1994). DNA strand breaks: The DNA template alterations that trigger p53-dependent DNA damage response pathways. Mol. Cell. Biol. *14*, 1815–1823.

Peifer, M., and Polakis, P. (2000). Wnt signaling in oncogenesis and embryogenesis-a look outside the nucleus. Science *287*, 1606–1609.

Polakis, P. (2000). Wnt signaling and cancer. Genes Dev. *14*, 1837–1851.

Reed, J.C. (1996). Balancing cell life and death: Bax, apoptosis, and breast cancer. J. Clin. Invest. *97*, 2403–2404.

Reed, J.C., and Ely, K. (2002). Degrading Liaisons: Siah structure revealed. Nat. Struct. Mol. Biol. *9*, 8–10.

Sadot, E., Simcha, I., Iwai, K., Ciechanover, A., Geiger, B., and Ben-Ze'ev, A. (2000). Differential interaction of plakoglobin and β-catenin with the ubiquitin-proteasome system. Oncogene *19*, 1992–2001.

Sadot, E., Geiger, B., Oren, M., and Ben-Ze'ev, A. (2001). Down-regulation of β-catenin by activated p53. Mol. Cell. Biol. *21*, 6768–6781.

Santelli, E., Leone, M., Li, C., Fukushima, T., Preece, N.E., Olson, A.J., Ely, K.R., Reed, J.C., Pellecchia, M., Liddington, R.C., and Matsuzawa, S. (2005). Structural analysis of Siah1-SIP interactions and insights into the assembly of an E3 ligase multiprotein complex. J. Biol. Chem. *280*, 34278–34287.

Shinkai, Y., Rathbun, G., Lam, K.P., Oltz, E.M., Stewart, V., Mendelsohn, M., Charron, J., Datta, M., Young, F., Stall, A.M., et al. (1992). RAG-2-deficient mice lack mature lymphocytes owing to inability to initiate V(D)J rearrangement. Cell *68*, 855–867.

Tanikawa, J., Ichikawa-Iwata, E., Kanei-Ishii, C., Nakai, A., Matsuzawa, S., Reed, J.C., and Ishii, S. (2000). p53 suppresses the c-Myb-induced activation of heat shock transcription factor 3. J. Biol. Chem. *275*, 15578–15585.

Tetsu, O., and McCormick, F. (1999). β-catenin regulates expression of cyclin D1 in colon carcinoma cells. Nature *398*, 422–426.

Vogelstein, B., Lane, D., and Levine, A.J. (2000). Surfing the p53 network. Nature *408*, 307–310.

Wahl, G.M., and Carr, A.M. (2001). The evolution of diverse biological responses to DNA damage: Insights from yeast and p53. Nat. Cell Biol. *3*, E277–E286.

Winston, J.T., Strack, P., Beer-Romero, P., Chu, C.Y., Elledge, S.J., and Harper, J.W. (1999). The $SCF^{\beta\text{-}TRCP}$-ubiquitin ligase complex associates specifically with phosphorylated destruction motifs in IκBα and β-catenin and stimulates IκBα ubiquitination in vitro. Genes Dev. *13*, 270–283.

Wu, L., and Strasser, A. (2001). "Decisions, decisions…": β-catenin-mediated activation of TCF-1 and Lef-1 influences the fate of developing T cells. Nat. Immunol. *2*, 823–824.

Xu, Y., Banerjee, D., Huelsken, J., Birchmeier, W., and Sen, J.M. (2003). Deletion of β-catenin impairs T cell development. Nat. Immunol. *4*, 1177–1182.

Zhang, J., Guenther, M.G., Carthew, R.W., and Lazar, M.A. (1998). Proteasomal regulation of nuclear receptor corepressor-mediated repression. Genes Dev. *12*, 1775–1780.

Zhou, B.B., and Elledge, S.J. (2000). The DNA damage response: Putting checkpoints in perspective. Nature *408*, 433–439.